www.lajss.org
Latin American Journal of Solids and Structures 2 (2005) 113–152

Split Hopkinson pressure bar techniques for characterizing soft materials

Bo Song and Weinong Chen

Schools of Aero/Astro and Materials Engineering, Purdue University, West Lafayette, IN 47907, USA

Abstract

Efficient usage of soft materials under impact loading conditions requires accurate and reliable descriptions of the high-rate mechanical responses of such materials, which motivates recent development of valid and efficient dynamic experimental techniques. Split Hopkinson pressure bar (SHPB) has been extensively used to characterize dynamic behavior of metallic materials, but less for soft materials because of experimental uncertainties associated with soft material characterization. This paper first presents major challenges encountered in Hopkinson bar experiments on soft materials, including weak transmitted signals, dynamic stress equilibrium, and constant strain rate, and then summarizes recent research efforts in the modifications to the conventional SHPB for obtaining valid and accurate stress-strain data for soft materials.

Keywords: split Hopkinson pressure bar (SHPB), soft material, dynamic property, stress equilibrium, constant strain rate

1 Introduction

Soft materials are typically referred to materials with low strength and stiffness, such as polymers, polymeric foams, and metallic foams. Although not artificially engineered, biological tissues may also be classified as soft materials based on their mechanical responses. Engineered soft materials are typically good shock mitigation and vibration isolation materials, which have been recently utilized in wide ranges of applications in aerospace, automotive, transportation, packaging, and other military and civil fields [26]. In these applications, the soft materials may be subjected to impact loadings such as crash, explosion, and high-speed collision. Understanding the mechanical responses of the soft materials under impact loading conditions leads to more efficient engineering applications and designs [79]. Furthermore, numerical simulations have been increasingly used in engineering designs, which require an accurate family of stress-strain curves at various strain rates to obtain realistic predictions of structural impact responses [72]. Reliable dynamic experiments on soft materials must be designed and carried out to determine such dynamic stress-strain curves before a strain-rate-dependent material model can be developed.

* Corresponding author E-mail: songb@ecn.purdue.edu Received 15 June 2005; In revised form 17 June 2005

As compare to quasi-static experiments, dynamic characterization of materials, especially soft materials, at high strain rates is still much more challenging since currently-available dynamic testing techniques have been less capable of obtaining reliable stress-strain data at high strain rates [17,28,35,36,45,66]. Developing efficient and accurate high-strain-rate experimental methods thus becomes necessary to obtain valid and accurate high-rate stress-strain curves.

Split Hopkinson pressure bar (SHPB) has been widely recognized as a highly efficient experimental technique to obtain families of stress-strain curves for engineering materials at high strain rates between 10^2 to 10^4 s^{-1} [25, 26, 33, 35, 36], since it was developed by Kolsky [31]. However, when the SHPB is used for characterizing the dynamic behavior of soft materials, the validity and accuracy of experimental data need to be carefully examined. As the soft materials commonly exhibit low modulus, flow stress, and mechanical impedance, the conventional SHPB has been demonstrated to be insufficient to obtain accurate stress-strain data for the soft materials such that it needs to be properly modified for testing such soft materials. Modifications to the SHPB for soft-material testing have been discussed and developed in recent decades, however, rarely systematically documented [8, 11, 26]. In this paper, we summarize the recent developments in the SHPB technique for characterizing soft materials.

2 Conventional SHPB technique

A conventional SHPB apparatus, which is schematically shown in Fig. 1, consists of a gas gun (or a launching device), a striker, an incident bar, a transmission bar, an energy absorption device, and a data acquisition system. The specimen is sandwiched between the incident bar and the transmission bar. The impact of the striker, which is commonly launched by compressed gas in the gas gun, on the end of the incident bar generates elastic waves in both the striker and incident bar. The elastic wave in the incident bar is called *incident wave*. When the *incident wave* travels through the incident bar to the specimen, due to the mismatch of mechanical impedances between the bar material and the specimen, part of the *incident wave* is reflected back into the incident bar as a *reflected wave* and the rest of the *incident wave* transmits through the specimen, which compresses the specimen at high rates, into the transmission bar as a *transmitted wave*. The incident and reflected signals are sensed by the strain gages on the incident bar whereas the transmitted signals are sensed by the strain gages on the transmission bar. All three signals are recorded with a digital oscilloscope or a computer.

During a SHPB experiment, the bars serve as sensors and thus must meet some strict requirements such that the data interpretation has minimum uncertainties. First, the pressure bars must remain elastic and the length should be sufficiently long, compared to the length of the incident wave to avoid overlapping of the waves [25]. Slender bars are recommended to minimize the effects of two-dimensional stress wave propagation in the bars. The ends of the bars in contact with the specimen must remain flat and parallel throughout the test [25]. In addition, the cross-sectional area of the specimen is always required not to exceed that of the

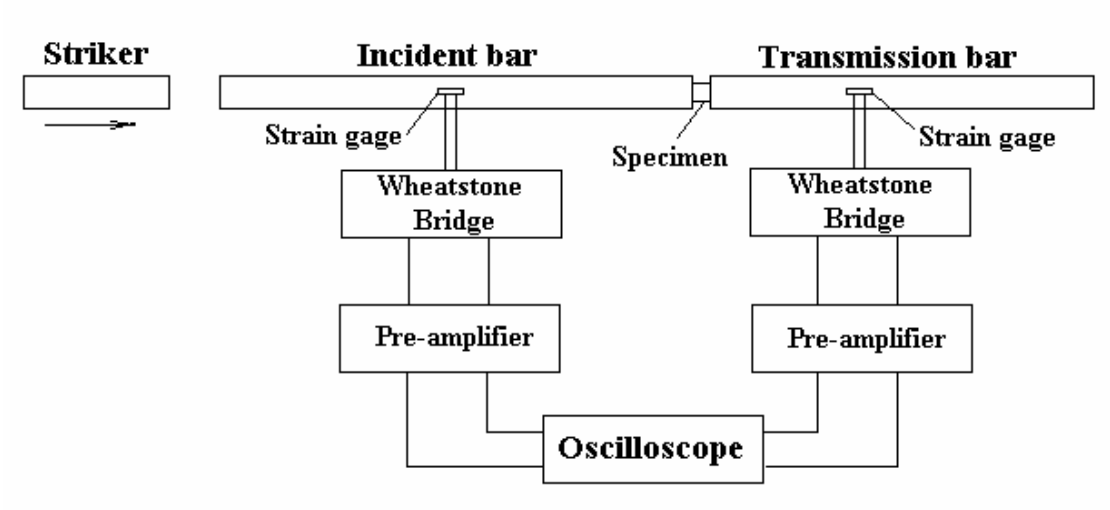

Figure 1: A schematic of conventional SHPB setup.

bars.

One-dimensional stress-wave analysis on the bars yields the strain rate, strain, and stress histories in the specimen [25],

$$\dot{\varepsilon} = \frac{C_0}{L_s} \left[\varepsilon_i (t) - \varepsilon_r (t) - \varepsilon_t (t) \right] \tag{1}$$

$$\varepsilon = \frac{C_0}{L_s} \int_0^t \left[\varepsilon_i (t) - \varepsilon_r (t) - \varepsilon_t (t) \right] dt \tag{2}$$

$$\sigma = \frac{A_0}{2A_s} E_0 \left[\varepsilon_i (t) + \varepsilon_r (t) + \varepsilon_t (t) \right] \tag{3}$$

where $\varepsilon_i (t)$, $\varepsilon_r (t)$, and $\varepsilon_t (t)$ are incident, reflected, and transmitted strain histories sensed by strain gages, respectively; A_0 is the cross-sectional area of the bars; E_0 and C_0 are Young's modulus and elastic bar wave speed in the bar material, respectively; A_s and L_s are initial cross-sectional area and length of the specimen, respectively. When the specimen is in a state of uniform stress,

$$\varepsilon_i (t) + \varepsilon_r (t) = \varepsilon_t (t) \tag{4}$$

Equations (1)-(3) can be simplified as

$$\dot{\varepsilon} = -2 \frac{C_0}{L_s} \varepsilon_r (t) \tag{5}$$

$$\varepsilon = -2 \frac{C_0}{L_s} \int_0^t \varepsilon_r (t) \, dt \tag{6}$$

$$\sigma = \frac{A_0}{A_s} E_0 \varepsilon_t (t) \tag{7}$$

Therefore the stress-strain data can be derived from the recorded strain gage signals in a SHPB experiment.

Equation (7) indicates that the stress in specimen is proportional to the transmitted signal, ε_t. When soft materials are tested using the SHPB, this transmitted signal may be too weak to be accurately sensed by the regular resistor strain gages on the metallic transmission bar, resulting in inaccurate measurements of stress in the specimen. The inaccurate stress data inevitably compromise the accuracy of stress-strain data for the material. In order to obtain accurate stress-strain responses for soft materials, the method of obtaining the transmitted signal in a SHPB needs to be modified.

Even though a transmitted signal with high signal-to-noise ratio is obtained, dynamic equilibrium of stress in specimen presents another major obstacle in obtaining reliable stress-strain data from a conventional SHPB experiment. Equations (5)-(7) are based on the assumption of dynamic stress equilibration in the specimen (Eq. (4)), which is not satisfied automatically when the specimen material is very soft. Dynamic stress equilibrium can be achieved quickly in a metallic or ceramic specimen due to relatively high wave speeds in those specimens. However, the stress state in a soft specimen may not be in equilibrium over the entire loading duration in a SHPB experiment on a soft material as the wave speeds in such materials are often very slow [8,11,26]. In a SHPB experiment, it takes several rounds of reflections in specimen for stress wave to "ring up" to a state of dynamic stress equilibrium. The non-equilibrated stresses in specimen during a SHPB experiment may lead to a drastic non-uniform deformation in specimen, which invalidates the experimental results for material property characterization [8].

Figure 2 shows high-speed images of a dynamic deformation process in a RTV630 rubber specimen in a conventional SHPB experiment. A trapezoidal pulse was produced in the incident bar and loaded on the rubber specimen with 12.60 mm in diameter and 12.70 mm in length. A digital high-speed camera was used to record the specimen deformation during dynamic loading at the rate of 80,808 frames per second (FPS). Figure 2 clearly shows that the specimen deformed non-uniformly during the experiment. The drastic non-uniform deformation in specimen demonstrates that the conventional SHPB experiment cannot produce valid dynamic properties of the rubber material.

When the tested specimen is a low-density foam material, this non-equilibrium situation in specimen may be worse. Figure 3 shows high-speed deformation process of an epoxy foam specimen loaded with a trapezoidal incident pulse produced in a conventional SHPB experiment. The epoxy foam column had a 10×10-mm^2 cross section and a 19-mm length. It is observed that the specimen started to fail from one end and the failure front traveled towards the other end. The existence of the failure front, which divides the specimen into compacted and uncompacted zones, confirms the drastic non-uniform deformation in specimen during the experiment. The resultant data in this case represent the structural behavior of a collapsing column instead of material behavior for this foam.

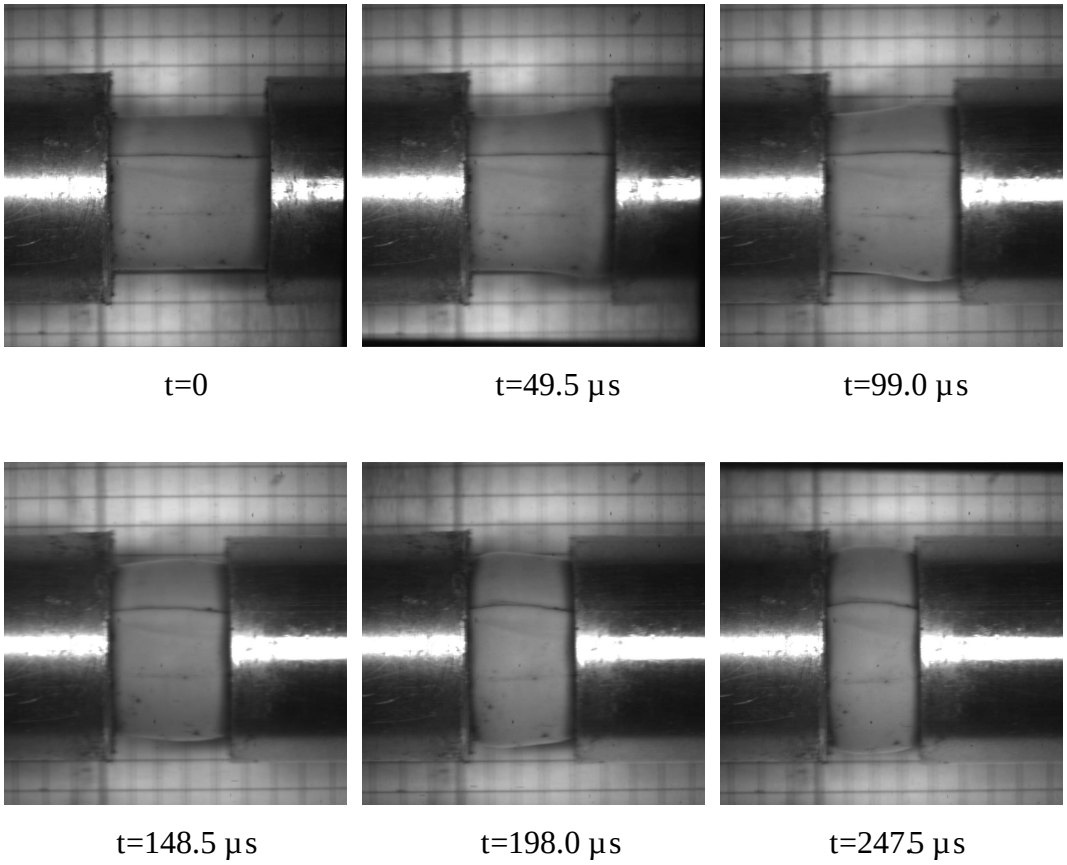

Figure 2: High-speed images of a RTV630 rubber specimen deforming dynamically in a conventional SHPB experiment.

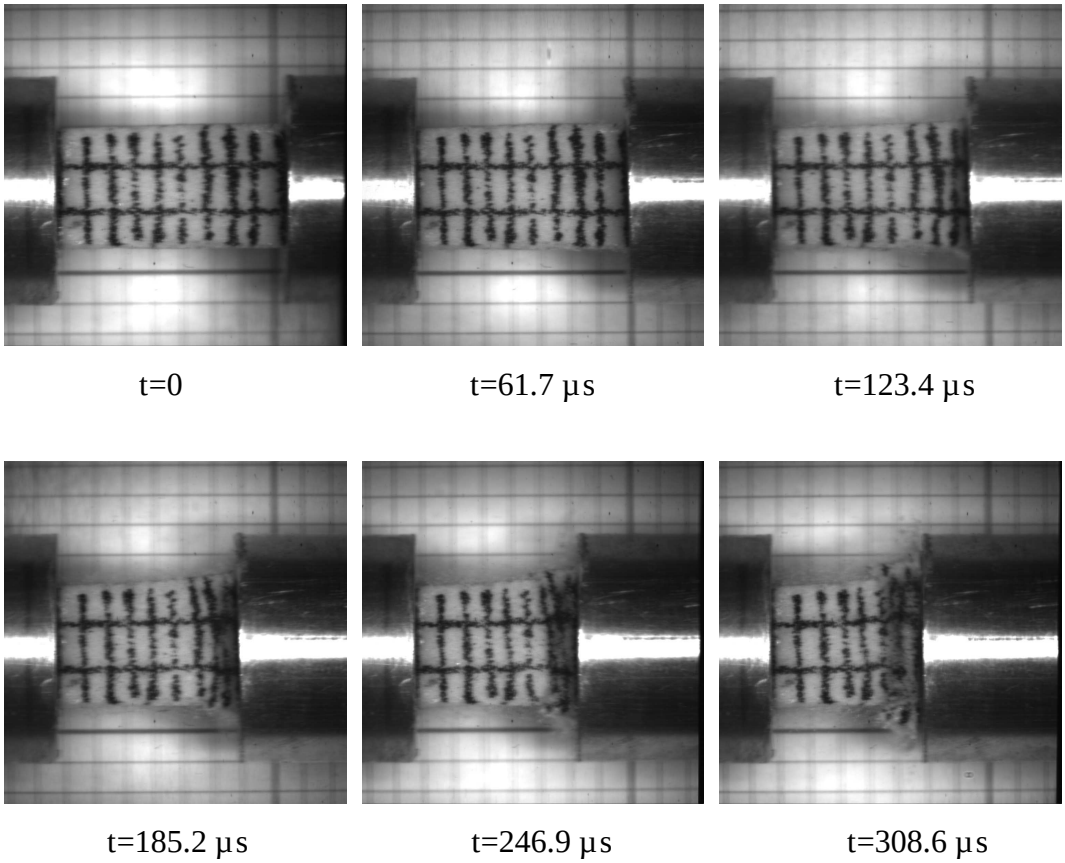

Figure 3: High-speed deformation of an epoxy foam specimen in a conventional SHPB experiment.

In both RTV630 rubber and epoxy foam cases, it is not possible to use the average deformation to represent the point-wise deformation in specimen. The resultant data obtained from such non-equilibrated stress states are not valid if Eqs. (5)-(7) are used to calculate the stress-strain curves. Equations (1)-(3) cannot be employed for data reduction either because the averaged stress and strain data do not represent the point-wise stress and strain states in specimen when the stresses in specimen are not equilibrated [8,11]. Therefore, in order to obtain valid dynamic properties of the specimen material, it is essential that this equilibrium state of stress be achieved over the duration of the experiment. This requires modifications to the conventional SHPB for testing soft materials.

Polymers and polymeric foams have been found to be strain-rate sensitive [8,11]. To examine the strain-rate effects and to report the stress-strain data as a function of strain rates, the strain rate level in an experiment needs to be accurately defined. In this case, a constant strain-rate deformation in the soft specimen is required in a SHPB experiment. In a conventional SHPB experiment, a trapezoidal incident pulse is generated regardless of specimen response. However, if the specimen does not deform at a constant flow stress, the strain-rate history will vary under a nearly constant loading pulse (trapezoidal pulse), which poses another challenge in the SHPB experiments on rate-sensitive materials [12, 15]. Under dynamic stress equilibrium, the value of engineering strain rate is proportional to the amplitude of reflected pulse (Eq. (5)). The reflected pulse thus must be maintained to a nearly constant value, which is not often achieved in a conventional SHPB experiment because of the work hardening characterization of the specimen material. In order to facilitate constant strain-rate deformation in specimen, the loading pulse profile in a SHPB needs to be modified.

The conventional SHPB in general offers mechanical tests at strain rates between 10^2 and 10^4 s^{-1} [35, 36]. It is difficult to conduct dynamic experiments on soft materials at relatively low strain-rates, which leaves scarcity of data in the intermediate strain-rate range of 10^0 to 10^2 s^{-1} [76, 77]. In this intermediate strain-rate range, the loading duration needs to be sufficiently long to obtain large deformations in specimens at such low strain-rate levels since many soft materials including rubbers and foams are capable of large deformations [76]. A conventional SHPB does not generate incident pulses with low amplitudes but long durations. However, it may become feasible after proper modifications to the conventional SHPB such that the applications of the Hopkinson bar technique may be extended to perform mechanical experiments on soft materials in the range of intermediate strain rates.

After dynamic stress-strain curves are obtained, the specimens after mechanical loading, in some cases, are desired to be collected for microstructural investigations [62, 63]. In order to build up an accurate relationship between the microstructures and macroscopic mechanical properties in specimen, loading histories need to be correlated to microstructure evolutions in specimens. However, in a conventional SHPB experiment on a soft material, the incident pulse is mostly reflected back due to the weak resistance from the soft specimen. This reflected pulse will be reflected back into the incident bar at the free striking end and will load the specimen again. The reloading process will repeat numerous times during an experiment and destroy

the one-to-one relationship between the loading history and the microstructure evolution inside the collected specimen after mechanical loading. Therefore, the conventional SHPB needs to be modified to ensure a single loading on specimen during the experiment for the purpose of microscopic investigations related to stress-strain data [36, 37].

In summary, when the conventional SHPB is used for testing soft materials, there are several uncertainties that may invalidate the resultant stress-strain data. The conventional SHPB should be properly modified in order to obtain valid stress-strain data for soft materials. The modifications to the conventional SHPB are presented in the following sections.

3 Modified SHPB for characterizing soft materials

In order to obtain valid and accurate stress-strain data for soft materials, the weak transmitted signal must be measured with a high signal-to-noise ratio. Furthermore, the soft specimen must be ensured to deform at a constant strain rate under dynamically equilibrated stresses during the experiment [8]. These three requirements (accurate transmitted signal measurement, dynamic stress equilibrium, and constant strain-rate deformation) are essential to ensure accurate stress-strain data for soft materials.

3.1 Sensing weak transmitted signal

When the SHPB is used to characterize soft materials with very low modulus and mechanical impedance, the data acquisition method needs to be carefully selected due to the possible weak transmitted signal. Gray and Blumenthal [26] provided a guideline of selecting bar material for soft-material testing. They pointed out that lower-impedance pressure bars are required to measure stress-strain responses of soft materials with high resolution. They recommended polymer and low-mechanical-impedance metallic bars [26].

In the past decade, polymeric bars, which have much lower mechanical impedance than metallic bars, have been employed to sense weak transmitted signals with sufficiently high signal-to-noise ratio [1, 5, 26, 46, 49, 70, 75, 78]. In addition to cast acrylic [49], polymethyl methacrylate (PMMA) and polycarbonate (PC) are mostly common materials selected as the bar material to test soft materials including polymeric foams and rubbers [1, 5, 46, 70, 75, 78].

Through employing such polymeric bars, the amplitude of the transmitted signal is significantly increased with high signal-to-noise ratio due to decreased mechanical impedance difference between the bar and specimen materials. However, the small impedance mismatch between the polymeric bars and the soft specimen extends the period of time to reach dynamic stress equilibrium in the specimen [22]. In addition, polymeric materials, unlike metals and alloys, do not exhibit perfectly linear elastic behavior, even within the range of small strains. These materials also exhibit significant stress-wave dispersion and attenuation due to their viscoelastic nature, which bring uncertainties into data reduction from viscoelastic bar experiments [1, 5, 46, 49, 70, 75, 78]. As a stress wave travels along a polymeric pressure bar, not only the wave amplitude decreases

due to attenuation, but also the wave shape becomes distorted because of dispersion such that the strain signal measured at a given position on the viscoelastic bar is not the same as that at the bar/specimen interface [26]. Thus the classic SHPB analysis cannot be applied to viscoelastic bars unless corrections are conducted based on a viscoelastic wave analysis in the polymeric bar material [1, 5, 46, 49, 70, 75, 78].

An accurate material model that describes viscoelastic response is necessary to be derived for the purpose of correcting the dispersion and attenuation of viscoelastic wave propagating in the polymeric bar material. Zhao and Gary [75, 78] used a wave profile recorded at one point on the incident bar as input data to a stress-strain model they proposed for the polymeric bar material. The model parameters were determined through comparison with the predicted and measured waves at another point on the incident bar. Sawas et al. [49] measured the strain or particle velocity at two different locations on a polymeric bar using a similar method. The strain measurements at the two positions were then deducted analytically to determine the model parameters for a viscoelastic description of the polymeric bars. Once the model parameters have been identified, the material models are capable of correction of wave dispersion and attenuation such that the measured strain signals at one position (strain gage location) on the bars can be correlated to the specimen/bar interfaces. Then the classic data-reduction analysis (Eqs. (5)-(7)) can be employed to calculate stress-strain data for the specimen. Sawas et al. [49] presented a detailed procedure of correcting the viscoelastic waves and calculating the stress-strain data in their paper.

The mechanical responses of viscoelastic bar materials are known to be sensitive to temperature and moisture levels. Furthermore, due to oxidation and ultraviolet radiation, the aging dependency of the viscoelastic bar materials also has to be accounted for during prolonged usage [26]. These factors (temperature, moisture and aging) significantly affect the determination of material parameters in modeling the viscoelastic bar materials. The effects of these factors on determination of material parameters in viscoelastic material models will inevitably affect the accuracy of stress-strain data for soft specimens tested with the viscoelastic polymeric bars.

To avoid such uncertainties caused by viscoelastic bars, low-impedance metallic bars, such as titanium [27], magnesium [26, 50], and aluminum bars [8], have been demonstrated to be good candidates for bar materials. Like using polymeric bars, the reduced mechanical impedance mismatch between the bar material and the specimen material increases the amplitude of the transmitted signal. However, the low-impedance metallic bar materials are less affected by environment.

Among the low-impedance metallic bar materials, the aluminum bars are the most commonly used for testing soft materials [8]. The use of aluminum bars has proved capability of accurately determining the mechanical responses for a number of polymeric materials. However, when the tested specimen is very soft, the aluminum bars might not be sufficient to provide a transmitted signal with high signal-to-noise ratio since the aluminum bars are only three times more sensitive than steel bars due to a reduced Young's modulus. Replacing the solid aluminum transmission bar with a hollow aluminum bar has been recommended by Chen et al. [13] to measure the weak

transmitted signal with a reasonable signal-to-noise ratio. Since the hollow transmission bar has much smaller cross-sectional area than the solid bar, the transmitted stress or strain signal that corresponds to a certain transmitted force is amplified by the hollow bar. In other words, this hollow bar works as a linear elastic stress/strain amplifier. In such a modified SHPB apparatus, the incident bar is a solid aluminum bar and the aluminum transmission bar is hollow. The classic data reduction equations for calculating strain rate and strain (Eqs. (5) and (6)) become more complicated due to the cross-sectional area mismatch between the solid incident and hollow transmission bars. The axial engineering strain of the specimen is [13]

$$\varepsilon(t) = \frac{C_0}{L_s}\int_0^t \left[\varepsilon_i(\tau) - \varepsilon_r(\tau) - \varepsilon_t(\tau)\right] d\tau = \frac{C_0}{L_s}\left(1 - \frac{A_i}{A_t}\right)\int_0^t \varepsilon_i(\tau)\, d\tau - \frac{C_0}{L_s}\left(1 + \frac{A_i}{A_t}\right)\int_0^t \varepsilon_r(\tau)\, d\tau \tag{8}$$

where A_i and A_t are the cross-sectional areas of the solid incident and the hollow transmission bars, respectively. The stress in specimen can still be calculated using Eq. (7). Equation (8) indicates that, when the hollow transmission bar is employed, the reflected pulse no longer represents the strain-rate history in specimen.

It has been recently found that employing the aluminum bars with high-accuracy transducers is more efficient and convenient to measure the weak transmitted signals. A quartz-crystal embedded aluminum transmission bar [10] has been developed to achieve high sensitivity for the weak transmitted signal while maintaining high impedance mismatch with soft specimen which is helpful to achieve dynamic stress equilibrium early. The quartz-crystal force transducer, which is placed in the middle of the aluminum transmission bar, is two to three orders of magnitude more sensitive than resistor strain gages. Quartz-crystal force transducers were used by previous investigators to measure dynamic force profiles [30, 69, 71]. Thin quartz crystal and aluminum disc are necessary to minimize the axial inertia-induced force signal superposed on the specimen response. The Boston Piezo-Optics X-cut circular piezoelectric quartz crystal force transducer used by Chen et al. [10] had a diameter of 19.050±0.025 mm (the same as the diameter of the bars) and a thickness of 0.254±0.025 mm. The piezoelectric constant of the quartz crystals is 2.3×10^{-12}C/N, as given by the manufacturer, which remains very linear up to pressures where dielectric breakdown occurs, and is not very sensitive to normal variations in environmental temperatures. The nearly matching mechanical impedance between the quartz crystals and the aluminum bar minimizes the disturbances to the one-dimensional wave propagation in the bar by introducing the quartz crystals. The output signals from the quartz crystal force transducers are commonly recorded using a high-speed digital storage oscilloscope through charge amplifiers.

Another efficient method for sensing a weak transmitted signal is to mount highly sensitive strain gages, e.g. semiconductor strain gages, on the aluminum or hollow transmission bar [11, 50]. Compare to the gage factor of ∼2.0 for regular resistor strain gages, the semiconductor strain gages have a much higher gage factor of ∼140, which indicates that a semiconductor strain gage is seventy times more sensitive than a regular resistor strain gage. The semiconductor strain gages, which provide sufficiently high accuracy to detect weak transmitted signals from most

soft materials, have been utilized in the Hopkinson bar experiments on polymeric foams and rubbers [11, 50]. It can be imagined that the resolution of the measured transmitted signal will be even higher when employing the semiconductor strain gages on a hollow aluminum transmission bar.

After the weak transmitted signal is accurately sensed, it becomes feasible to monitor the dynamic stress equilibrium process in a soft specimen during a SHPB experiment.

3.2 Detecting dynamic stress equilibrium process

3.2.1 Criteria for dynamic stress equilibrium

Criterions for stress equilibrium have recently been developed. The basic principle of these criterions is to compare the forces (or stresses) at both ends of specimen.

Parry et al [42] defined a "stress equilibrium factor" σ_{EQ} as

$$\sigma_{EQ} = \frac{\sigma_T}{\sigma_I + \sigma_R} \tag{9}$$

where σ_I, σ_R, and σ_T correspond to the incident, reflected, and transmitted stresses in a SHPB experiment. The stress equilibrium is perfectly achieved when the value of σ_{EQ} reaches unity.

Ravichandran and Subhash [47, 68] used another parameter, $R(t)$,

$$R(t) = \left| \frac{\Delta\sigma(t)}{\sigma_m(t)} \right| \tag{10}$$

which is the ratio of stress difference ($\Delta\sigma(t)$) at both faces of the specimen to the mean value ($\sigma_m(t)$) within the specimen to evaluate the proximity to stress equilibrium in specimen. The specimen is recognized to be in stress equilibrium when the value of $R(t)$ approaches zero. This parameter has been recently employed to evaluate the stress equilibrium process in the SHPB experiments [32, 47, 52, 58, 68].

Zencker and Clos [74] also presented the same formulation of the relative stress difference ratio, D,

$$D = 2 \left| \frac{\sigma_{zz}^{(a)} - \sigma_{zz}^{(c)}}{\sigma_{zz}^{(a)} + \sigma_{zz}^{(c)}} \right| \tag{11}$$

as the criterion of stress equilibrium, where $\sigma_{zz}^{(a)}$ and $\sigma_{zz}^{(c)}$ are axial stresses at both ends of specimen. They considered the specimen in the stress uniformity when the relative stress difference ratio, D, is smaller than 0.05.

Song and Chen [54] used a similar stress equilibrium parameter of $\Delta F/F_{aver}$ in their analysis of dynamic stress equilibration in SHPB tests on soft materials, where ΔF and F_{aver} are the difference and mean values of axial forces at the two ends of specimen, respectively. They also concluded that the specimen can be considered to be in dynamic equilibrium when the value of $\Delta F/F_{aver}$ is less than 0.05.

In summary, the state of stress equilibrium in specimen can be simply evaluated after forces (or stresses) at both ends of specimen are accurately measured.

3.2.2 Monitoring dynamic stress equilibrium process

The stresses at the both ends of specimen may be calculated using conventional methods which are so-called 2-wave and 1-wave methods [25],

$$\sigma_1 = E_0 \left(\varepsilon_i + \varepsilon_r\right) \tag{12}$$

$$\sigma_2 = E_0 \varepsilon_t \tag{13}$$

where σ_1 and σ_2 are the stresses in the bars at the front and back ends of specimen, respectively. As long as the incident (ε_i), reflected (ε_r), and transmitted (ε_t) signals are recorded, the stress equilibrium process can be monitored in a conventional SHPB experiment. However, when the conventional SHPB is used for testing soft materials, the low strength of the soft materials and high mechanical impedance mismatch between the bar and the specimen materials result in nearly the same (reverse symbol) reflected pulse as the incident pulse and a very weak transmitted signal [8]. This will lead to significant errors in calculation of stress at the front end of specimen using difference between the nearly-same incident and reflected pulses (Eq. (12)) even though the weak transmitted signal may be recorded with highly sensitive bars or transducers as described in Section 3.1 [8]. It is thus often not feasible to use Eq. (12) to calculate the force (or stress) at the front end of specimen when testing a soft material. In order to evaluate stress equilibrium process in a soft material, the force (or stress) at the front end of specimen needs to be accurately measured.

An efficient method to obtain the force (or stress) at the front end of specimen is direct measurement with a highly sensitive transducer which is similar to that for detecting the weak transmitted signal. Chen et al. [10] attached a pair of quartz crystal force transducers, which are introduced in Section 3.1, to the specimen ends of incident and transmission bars (Fig. 5). The mechanical impedance of the quartz-crystal transducers is very close to that of the aluminum bars, which ensures that the introduction of the quartz-crystal transducers does not affect the one-dimensional wave propagation in the bars [10]. To prevent the large lateral expansion of the soft specimen during axial compression from damaging the brittle quartz-crystal disks, a thin aluminum disk with the same diameter as the quartz disk was placed on each of the quartz-crystal disks. The aluminum disks also serve as an electrode to collect charges from the quartz crystal transducers.

It is noted that the quartz-crystal transducer itself and the attached aluminum disk may bring additional inertia stress into the recorded signal. Casem and his colleagues [3,4] observed that the stress measured by the quartz-crystal transducer on the incident bar often contains a substantial acceleration component, i.e., a significant peak-like portion of the signal. This peak-like signal recorded by the transducer is due to inertia and not a representative of the stress in the specimen. When the inertial stress is high in comparison to the "applied" stress, significant errors occur.

It will be erroneous to evaluate the stress equilibrium process in specimen when such quartz-crystal transducers are employed without corrections to monitor stress equilibrium process in specimen. Hence, the inertial stress needs to be compensated. Similar to the compensation of inertia stress in commercial piezoelectric gages, the inertia stress of the quartz-crystal transducer and the attached aluminum disk in a quartz-crystal embedded SHPB can also be compensated for. Casem et al. [3] used three quartz-crystal transducers together to effctively eliminate the additional inertia stress.

Comparison of the signals from the quartz crystal force transducers embedded at both ends of specimen facilitates a direct monitor of dynamic stress equilibrium process in specimen.

3.2.3 Factors to affect dynamic stress equilibrium

After the stress equilibrium process is monitored directly, it becomes possible to determine the key factors that affect the dynamic stress equilibration in SHPB experiments on soft materials.

Dynamic stress equilibrium is achieved only after waves in the specimen traverse it several times, causing the specimen to "ring up" to a nearly uniform stress under a step loading [25]. In experiments on materials that do not deform at a constant flow stress, the loading pulse cannot be a step. The profile of the incident pulse must be adjusted according to specimen response to achieve constant strain rates. The "ring up" in these cases becomes an ever-going process. The specimen is never in a true equilibrium state. However, as the mean stress in the specimen keeps increasing, the relative error caused by the ringing waves becomes relatively less and less [54]. Since the "ring up" process involves stress waves propagating inside the specimen, the wave speed in material is one of important factors which determine the time required for a specimen to reach dynamic stress equilibrium: the process is faster in a specimen with a high wave speed than in one with a low wave speed. Unfortunately soft materials often possess very slow wave speeds, which increase the time necessary to achieve dynamic stress equilibrium in a soft specimen with a certain thickness.

Since the wave speed in a certain material is considered to be constant, which cannot be changed during the experiment, specimen thickness naturally becomes a critical factor that affects the dynamic stress equilibration in soft materials. A thin specimen can shorten the time of dynamic stress equilibrium. In addition, the attenuation of stress wave is less significant when traveling through thin specimens [64].

Kolsky [31] pioneered the study on the thickness effects on the dynamic compressive stress-strain behavior of polythene material and found that the peak strength significantly depended on specimen thickness. In his original work, Kolsky [31] pointed out that a thick specimen would invalidate the assumption that the axial stresses on both sides of the specimen were nearly equal. Dioh et al. [18] also investigated the effects of specimen thickness on the mechanical properties of glassy polymers. The fact that the specimen strength decreased with increasing specimen thickness at the same strain rate showed that a thick specimen of soft material is not suitable for material property determination. A thick specimen indeed acts as a shock absorber, which

is a structure and is not a representative volume for material property testing. Gray et al. [27] performed SHPB experiments on Adiprene L-100 rubber with several thicknesses and showed that dynamic equilibrium was achieved only during the later stages of the experiments. Chen et al. [8] employed quartz-crystal transducers described in Section 3.2.2 to investigate the thickness effects in RTV630 rubber specimens. The specimen thickness was varied from 12.7 mm to 1.53 mm. In conventional SHPB experiments, the 12.7-mm-thick specimen was never in a state of dynamic stress equilibrium over the entire loading duration. When the specimen thickness was reduced, the force history profiles at both ends of specimen were very similar. However, the desired dynamic stress equilibrium was never achieved even though the specimen thickness was reduced to 1.53 mm.

Song and Chen [54] also extensively investigated the effects of specimen thickness on dynamic stress equilibrium for both RTV630 and ethylene-propylene-diene monomer (EPDM) rubber specimens. Under the same ramp loading (constant loading rate) condition, they conducted SHPB experiments on RTV630 and EPDM rubbers with various specimen thicknesses. Figure 4 shows the dynamic stress equilibrium processes in EPDM rubber specimens. Note that Eq. (10) was used to evaluate the dynamic stress equilibrium processes in Fig. 4. It is found that, at the loading rate of 8.15×10^5 MPa/s, the stress equilibrium was not achieved in specimens during the early stage of loading. This violation for stress equilibrium became more significant for thicker specimens. Stress equilibrium in a thick soft specimen may never be reached during the entire loading history. When the specimen thickness was reduced to 1.60 mm, the stress equilibrium was nearly achieved at 160 μs after initial loading. Similar results were also been obtained in RTV630 rubber experiment.

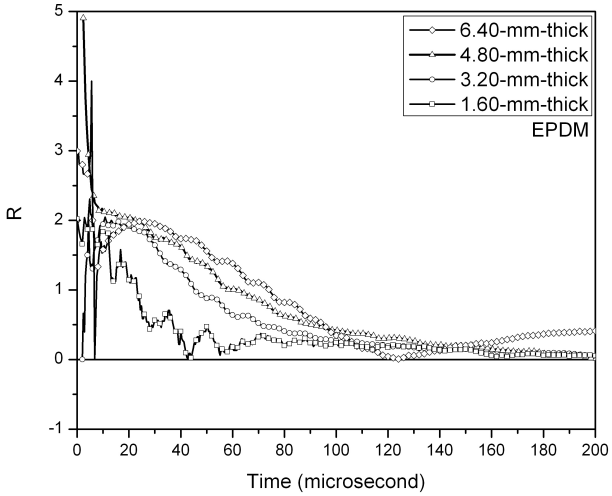

Figure 4: Specimen thickness effects on dynamic stress equilibrium in EPDM rubber specimens.

Using a thinner specimen will therefore facilitate a quicker process of equilibrium. However, the effects of interfacial friction between the specimen and the bars may become more significant. In the design of a dynamic experiment for soft material property determination, it is thus necessary to select a properly reduced specimen thickness.

It has been demonstrated that, even though a thin specimen is used, the dynamic stress equilibrium may not be achieved when the incident loading rate is very high [8]. The loading rate of the incident pulse has been found to significantly affect the dynamic stress equilibrium in a specimen with a certain thickness [54].

Wu and Gorham [73] pointed out earlier that increasing the rise time of the loading pulse could benefit dynamic stress equilibrium in the specimen. Chen et al. [8] found that the dynamic stress equilibrium could be achieved early when a pulse shaping technique (Fig. 5) was employed to facilitate different loading rates. This is because the pulse shaping technique decreased the loading rate (or increased the rise time) in the incident pulse. Without pulse shaping technique, dynamic stress equilibrium was never achieved in specimen even when a 1.53-mm-thick RTV630 rubber specimen was selected. However, dynamic stress equilibrium was found to be achieved in the 1.53-mm-thick RTV rubber specimen after the loading rate was decreased through the employment of a pulse shaper. Their results indicate that the loading rate of incident pulse plays a key role in achievement of dynamic stress equilibrium in soft specimens.

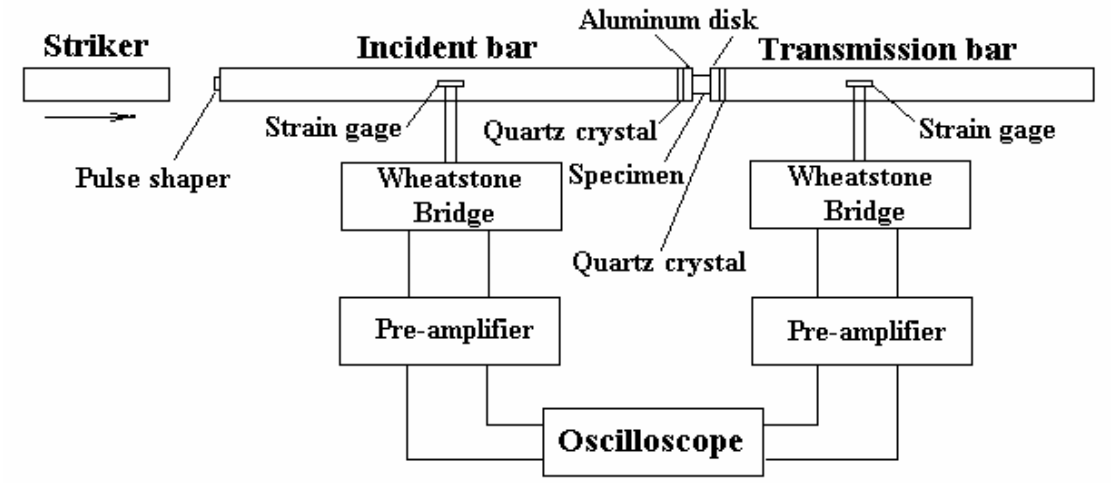

Figure 5: A schematic of the modified SHPB for soft-material testing.

Song and Chen [54] quantitatively investigated the effects of loading rate on dynamic stress equilibrium. They fixed the EPDM rubber specimen thickness at 1.60 mm and then varied the loading rate of the incident pulse from 1.45×10^6 to 6.69×10^4 MPa/s through pulse shaping technique that will be described in the following section. Figure 6 shows the incident loading rate effects on dynamic stress equilibrium in the 1.60-mm-thick EPDM rubber specimens. Since

the loading duration varied for various loading-rate experiments, the time axis (X-axis) in Fig. 6 was normalized by the total loading duration for each experiment. It is observed that, at the loading rates in the order of 10^6 MPa/s, the stress in the 1.6-mm-thick EPDM rubber specimen was never in a state of uniform during the experiment. When the loading rate was decreased one order of magnitude, the stress state in the specimen was close to be in equilibration. The stresses in specimen were nearly equilibrated after normalized time of 0.4 at the lowest loading rate of 6.69×10^4 MPa/s. Therefore, for a specimen of a certain thickness, the loading rate significantly affects the dynamic stress equilibrium process in the specimen.

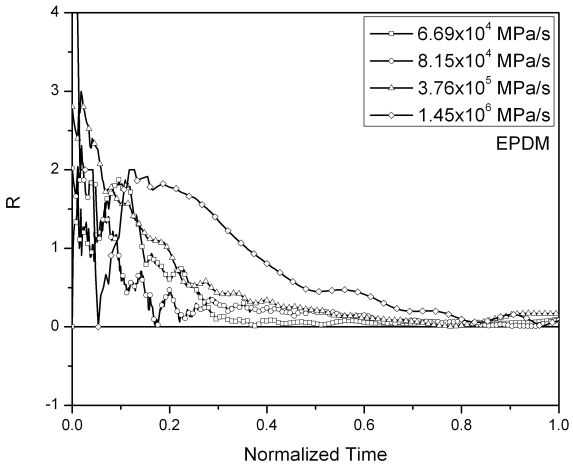

Figure 6: Loading rate effects on dynamic stress equilibrium in EPDM rubber specimens.

Besides the specimen thickness needs to be properly selected, the loading rate of the incident pulse is also required to be properly controlled to subject the specimen to a dynamic stress equilibrium state as early as possible. Both specimen thickness and loading rate effects on the stress equilibrium were modeled by Song and Chen [54].

3.3 Pulse shaping technique for dynamic stress equilibrium and constant strain-rate deformation in soft specimens

For a specimen with a certain thickness, the loading rate of incident pulse becomes the only controllable parameter to achieve dynamic stress equilibrium in a soft specimen. The loading rate of incident pulse can be adjusted through control of slope in incident pulse. The initial loading rate of incident pulse is especially critical to subject the specimen to stress equilibrium early. In addition to dynamic stress equilibrium, the profile of incident pulse needs to be controlled in order to obtain constant strain-rate deformation in soft specimens. As mentioned earlier, a trapezoidal incident pulse, which is typically produced in a conventional SHPB experiment, is

not capable of achieving constant strain-rate deformation for materials without constant flow stresses. In order to ensure the specimen deforms at a constant strain rate under dynamically equilibrated stresses to obtain valid stress-strain data, both initial loading rate and profile of incident pulse are required to be precisely designed. Pulse shaping technique has been developed and found to be a good method to facilitate such modifications to both initial slope and profile of incident pulse in a SHPB experiment [23, 37].

3.3.1 Introduction to pulse shaping technique

The pulse shaping technique for Hopkinson bar experiments was originally discussed three decades ago. The original motivations for the pulse shaping technique were to reduce the dispersion of waveforms such that smooth pulses were generated to improve the accuracy and resolution of the stress-strain curves [16, 19].

Conical strikers have been found to generate smooth pulses as well as to facilitate early dynamic stress equilibrium in brittle specimens [16]. In addition, a three-bar technique that employs a low-strength martensitic stainless steel bar as a pre-loading bar in front of the incident bar in a SHPB experiment can also efficiently eliminate the high-frequency oscillations such that the accuracy of the resultant stress-strain curve was improved [43]. This three-bar technique was originally developed by Ellwood et al. [20] two decades ago. Besides the pre-loading bar, Ellwood et al. [20] placed an additional specimen between the pre-loading bar and the incident bar as a dummy specimen. The best material for the dummy specimen was proposed to be the same as that of the actual test specimen for the purpose of maintaining constant strain-rate deformation in specimen. It has been recently found that the pre-loading bar could be removed and that employing only the dummy specimen at the end of incident bar on which the striker impacts was capable of facilitating constant strain-rate deformation in a SHPB experiment [2]. This method is simpler than the three-bar technique. It should be noted that these pulse-shaping techniques facilitate not only early dynamic stress equilibrium but also constant strain-rate deformation in specimen in a nearly dispersion-free SHPB experiment.

Similar to the dummy specimen placed at the impact end of the incident bar, another alternative pulse shaping technique is to place a "tip" material between the striker and the incident bar. The tip material was commonly a disk (sometimes a tube), which was attached to the impact end of the incident bar. The tip material could be made from paper, aluminum, copper, brass, stainless steel, etc. Besides reducing the oscillation of incident pulse [21, 73], the tip material has recently been used to generate a constant strain-rate experiment under dynamic stress equilibrium [29, 68].

Among the pulse shaper materials, copper disks have recently been extensively used in SHPB experiments to obtain valid and accurate data on materials [38, 39, 48, 61, 67]. The advantage of using a well-known material as pulse-shaping material lies in the capability of generating a variety of desired pulses that are necessary to subject the specimen to different constant strain rates under dynamic equilibrium. Quantitative analysis of generating controlled incident pulses

in a SHPB experiment was performed by Nemat-Nasser et al. [37] using OFHC (oxygen-free, high-purity copper) as a pulse shaper. More recently, Frew et al. [23,24] developed pulse-shaping models which have been applied to Hopkinson bar testing of linear elastic and bilinear elastic-plastic materials, such as rocks and work-hardening materials. Both analytical and experimental results indicate that the copper disks are simple but efficient to facilitate constant strain-rate deformations as well as dynamic stress equilibriums in specimens for various materials including soft materials. These pulse-shaping models provide guidelines for pulse shaper design in SHPB experiments.

3.3.2 Pulse shaping design in SHPB experiments for soft materials

As mentioned earlier, besides providing nearly oscillation-free pulses, the pulse shaping technique is used 1) to decrease initial incident loading rate (increase the rise time of the incident pulse) to facilitate early dynamic stress equilibrium; 2) to control the profile of the incident pulse to ensure the constant strain-rate deformation in specimen.

Employing a pulse shaper at the impact end of incident bar has been demonstrated to significantly increase the rise time of the incident pulse. However, modification of the incident pulse profile requires proper choice of the material and precise design of the dimensions of the pulse shaper to facilitate constant strain-rate deformations under dynamically equilibrated stresses in specimens. The desired profile of the incident pulse varies for testing various materials at different strain rates depending on the mechanical response of the tested material. In a SHPB experiment, under dynamic stress equilibrium, the reflected pulse represents the strain-rate history in specimen (Eq. (5)) if the incident and transmission bars have the same mechanical impedance. The transmitted signal, which is used to calculate the stress history in specimen, implies the stress-strain profile for a constant strain rate test. In order to maintain constant strain-rate deformation in specimen, a reflected pulse with a plateau is desired after dynamic stress equilibrium is achieved. The profile of the incident pulse is expected to be similar to that of the transmitted signal except for a higher amplitude to obtain a nearly plateau in the reflected pulse (constant strain rate). Thus the profile of the incident pulse needs to be accurately designed to facilitate a plateau in reflected pulse depending on the profile of the transmitted signal.

We provide a guideline for pulse shaping design in the SHPB testing of soft materials, which exhibit different mechanical responses, through the following examples. In these examples, the bar system with pulse shaping that is illustrated in Fig. 5 is employed unless additionally declared. The bars which are made of aluminum alloy had a common diameter of 19.05 mm.

Since we only focus on the Hopkinson bar technique for testing soft materials in this paper, the detailed discussions of material properties are not offered. Readers may refer to the related references for details in characterization of the soft materials.

Example 1. Pulse Shaping Design for Testing An Elastic-Brittle Foam. An epoxy syntactic foam is a typical elastic-brittle material, which exhibits a nearly linear response with

a small failure strain. To facilitate a constant strain-rate deformation in such a material, a loading pulse with a constant stress rate, i.e., a ramp profile, is necessary. A variation in the slope of the ramp produces a different strain rate in the specimen. Figure 7 presents two sets of incident, reflected, and transmitted signals at the strain rates of 300 and 550 s^{-1} recorded in pulse-shaping SHPB experiments on the epoxy syntactic foam [57]. The incident pulses were obtained through employing C11000 copper disks as pulse shapers. Varying the dimensions of the pulse shaper and the striking velocity produced incident pulses with different slopes shown in Fig. 7 to facilitate compression tests at various constant strain rates. It is observed that, after the pulse shapers were employed, the profiles of the incident pulses generated were nearly linear, which are quite different from those trapezoidal profiles obtained in conventional SHPB experiments. Such profiles of incident pulses ensured that the specimens deformed at nearly constant strain rates, which are proportional to the reflected pulses in Fig. 7 under dynamically equilibrated stresses. The processes of dynamic stress equilibrium are shown in Fig. 8. Figure 8 indicates that the dynamic stress equilibrium in specimens was achieved within most of loading durations for both tests due to the modified loading profiles through pulse-shaping. The strain-rate histories in specimens are shown in Fig. 9. The strain rates were observed to be maintained at constants within most of loading duration until the specimens failed (Fig. 9). It is noted that the strain rate is not constant until $\sim$50 μs after the specimen is loaded. In a dynamic experiment, this initial non-constant strain rate is inevitable because it takes time for the strain rate to increase from zero to a finite value. The focus of the experimental technique in this case is moved to maintain a constant strain rate at higher loading levels where significant deformation and failure behavior of the specimen are recorded, as shown for $t > 50\mu s$ in Fig. 9. The sharp rise in the strain rate (550 s^{-1}) history in Fig. 9 indicates that the specimen has failed and lost its load-carrying capacity, resulting in an increase in the incident bar/specimen interface velocity.

When this brittle material is compressed under uniaxial strain conditions, the profile of incident pulse is necessary to be redesigned as the stress-strain response of the material under uniaxial strain conditions is different from that under uniaxial stress conditions. Due to the possible increase of specimen strength under uniaxial strain conditions, a 12.7-mm-diameter maraging steel bar was employed to conduct the confinement experiments on the epoxy syntactic foam. The specimen had the same diameter (12.70 mm) as the bars and was surrounded with a snug-fit steel sleeve to confine the lateral deformation when the specimen was compressed axially [62]. Since the lateral displacement of specimen is restricted, the brittle material no longer exhibits typical brittle response under lateral confinement. Figure 10 shows the incident, reflected, and transmitted signals obtained from a SHPB confinement experiment on the epoxy syntactic foam. The transmitted signal exhibits elastic-plastic-like response under lateral confinement. The bi-linear profile in the incident pulse is thus necessary to facilitate constant strain-rate deformation under dynamic stress equilibrium, as shown in Fig. 11. Figure 11 indicates that the confined specimen was in dynamic stress equilibrium from 30 μs after initial loading while the strain rate reached to a nearly constant level of $\sim$1300 s^{-1}. The stress-strain curve at the strain rate of

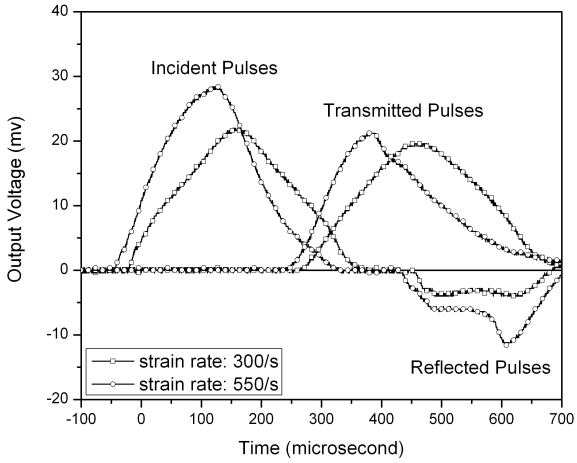

Figure 7: Typical incident, reflected, and transmitted signals at two strain rates obtained from pulse-shaping SHPB experiments on epoxy syntactic foam specimens.

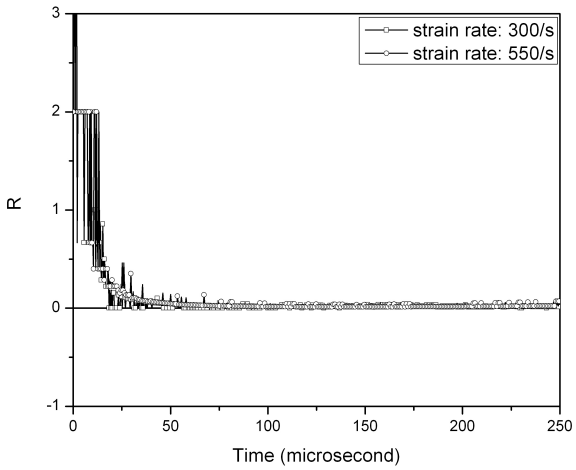

Figure 8: Dynamic stress equilibrium processes in epoxy syntactic foam specimens.

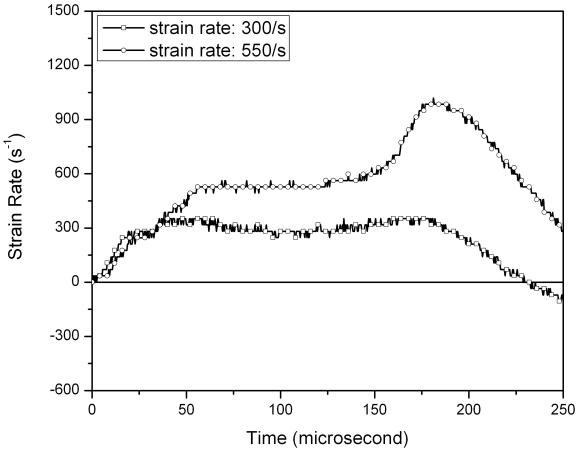

Figure 9: Strain-rate histories in epoxy syntactic foam specimens.

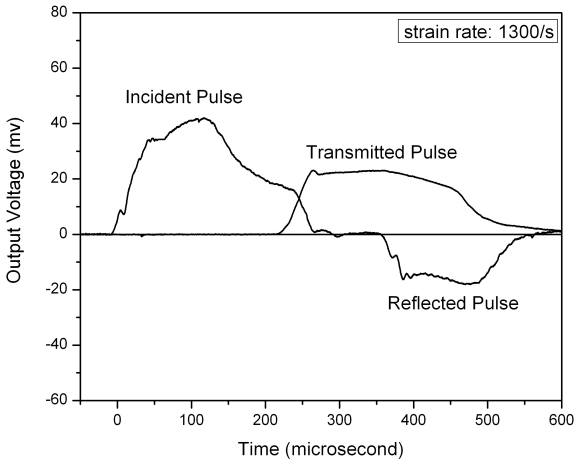

Figure 10: Incident, reflected, and transmitted pulses in a modified SHPB experiment on an epoxy syntactic foam specimen under lateral confinement.

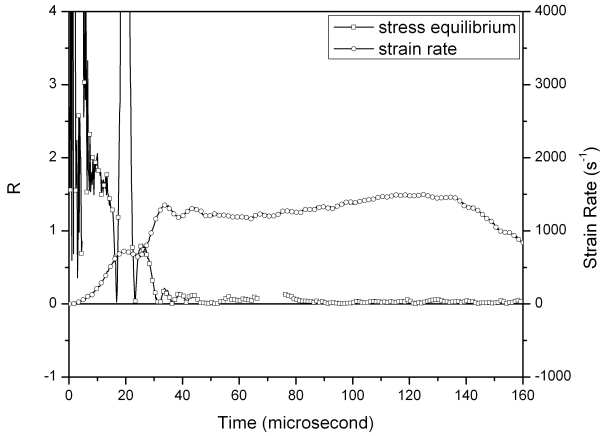

Figure 11: Dynamic stress equilibrium and strain-rate history in the epoxy syntactic foam specimen under lateral confinement.

1300 s^{-1} under lateral confinement was calculated under regular Hopkinson bar data reduction procedure (Eqs. (5)-(7)). It is noted that, under lateral confinement, the interfacial friction between the specimen and the steel sleeve has been neglected in the data reduction procedure. The resultant stress-strain curves at various dynamic strain rates under both uniaxial stress and uniaxial strain conditions are shown in Fig. 12. The profiles of stress-strain curves changed when the loading conditions changed from uniaxial stress to uniaxial strain. In addition to confinement effects, Figure 12 indicates strain-rate effects for this material under both uniaxial stress and strain loading conditions. The detailed strain-rate and confinement effects of this material can be found in Refs. [62]. Moreover, temperature effects of this material has also been investigated and discussed in Ref. [63].

Example 2. Pulse Shaping Design for Testing Rubbers. When the specimen is a rubber or rubber-like material, the profile of incident pulse needs to be changed accordingly because of nonlinear large deformation characterization of the rubber or rubber-like materials [7, 8, 14, 51]. Figure 13 shows a set of incident, reflected, and transmitted signals at strain rate of 4700 s^{-1} from the SHPB experiments on an EPDM rubber. An annealed C11000 copper disk was employed as the pulse shaper in the experiment. The incident pulse was observed to possess a rise time as long as 100 μs. This long rise time is necessary to ensure the specimen to achieve a state of uniform stress during the experiment. The dynamic stress equilibrium process in the EPDM rubber, which was monitored by the quartz transducers, is shown in Fig. 14. Figure 14 clearly indicates that the specimen was in dynamic stress equilibrium over the entire loading duration. However, the strain rate was achieved to a constant after 100 μs due to the long rise time in the incident pulse. The engineering stress-strain curves for this EPDM rubber at the strain rates from 2100 to 4700/s are shown in Fig. 15, where significant strain-rate effects are observed.

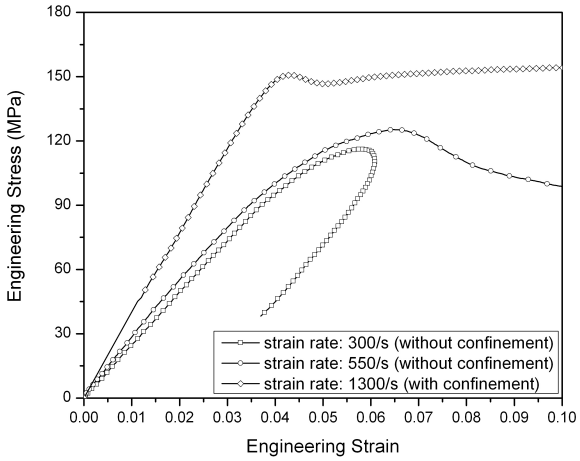

Figure 12: Engineering stress-strain curves at various strain rates of the epoxy syntactic foam with and without lateral confinement.

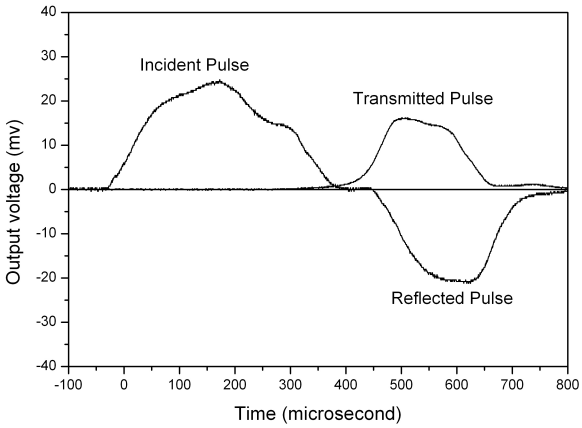

Figure 13: Incident, reflected, and transmitted pulses in a modified SHPB experiment on an EPDM rubber specimen.

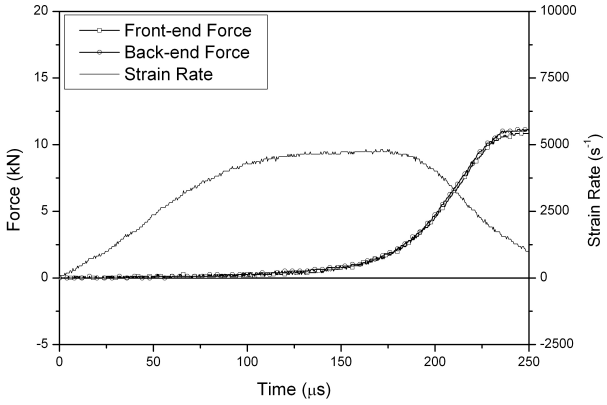

Figure 14: Dynamic stress equilibrium and strain-rate history in the rubber specimen.

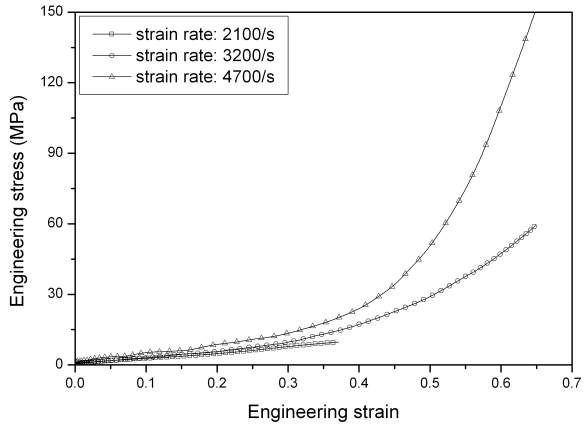

Figure 15: Engineering stress-strain curves of the EPDM rubber at various dynamic strain rates.

Rubber materials may be considered as volume-incompressible. When the rubber specimen is subject to external loading under uniaxial strain or multiaxial stress conditions, the stress in the specimen will increase drastically such that the incident pulse is required to be nonlinearly increased to maintain the constant strain-rate deformation in specimen [6,53]. Figure 16 shows the typical incident, reflected, and transmitted oscilloscope records in a SHPB experiment on the rubber specimen under nearly uniaxial strain conditions [53]. It is observed that the EPDM rubber exhibited similar stress-strain profile but much higher stresses at certain uniaxial strains, as compared to those obtained under uniaxial stress conditions. Most of the incident pulse was transmitted into the transmission bar as the transmitted pulse and only a small portion of incident pulse was reflected back as the reflected pulse. The significantly increased stress in specimen requires more input kinetic energy to maintain nearly constant strain-rate deformation. As indicated in Fig. 16, the incident pulse profile is quite different from that in Fig. 13. However, this modified profile ensured that the specimen deformed at a nearly constant strain rate, as shown in Fig. 17. In the meantime, the stress was in an uniform state within most of loading duration (Fig. 17), which confirms the validity of resultant stress-strain data. The stress-strain curves at various strain rates for the EPDM rubber under uniaxial strain conditions are shown in Fig. 18. Besides nonlinear stress-strain response for this rubber, significant strain-rate effects are observed under uniaxial strain conditions.

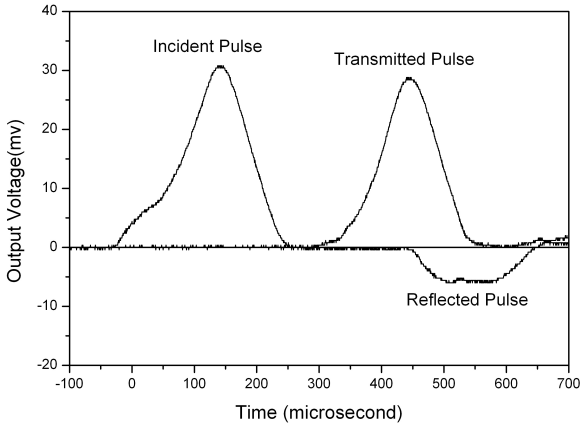

Figure 16: Incident, reflected, and transmitted pulses in a modified SHPB experiment on an EPDM rubber specimen under nearly uniaxial strain conditions.

Example 3. Pulse Shaping Design for Testing Low-Density Foam Materials. In general, the pulse shaping design for testing regular polymeric foams is not the same as those for testing brittle foam and rubbers described above because the regular polymeric foams have unique elastic-cell collapsing-densification stress-strain characterization [8,9,11,58,64]. In addition, the

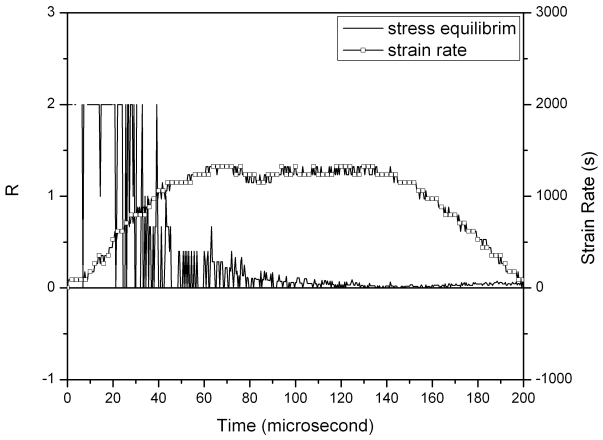

Figure 17: Dynamic stress equilibrium and strain-rate history in the rubber specimen.

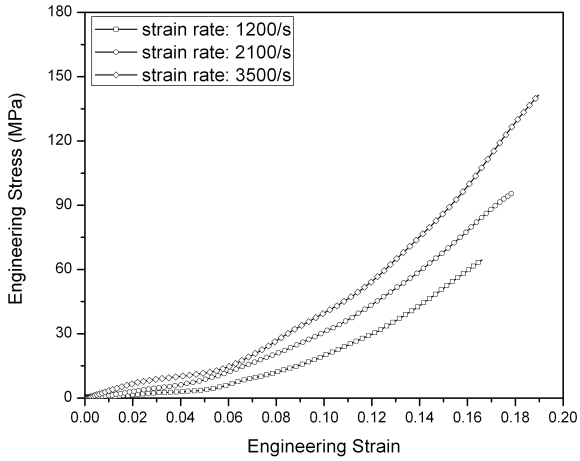

Figure 18: Engineering stress-strain curves of the EPDM rubber at various dynamic strain rates under nearly uniaxial strain conditions.

very low mass density and slow wave speed in the regular polymeric foams result in drastically reduced mechanical impedance, resulting in more severe impedance mismatch between the foam materials and the bars. Nearly all of the incident pulse is reflected back and the transmitted pulse is too weak to be clearly detected when regular resistance strain gages are used to sense the signals. In this case, the profile of incident pulse may not be necessary to be similar to the transmitted pulse since the amplitude of the later is nearly negligible when compared to the former. Instead, the profile of incident pulse is desired to be a trapezoidal but without high-frequency oscillations profile for the purpose of achievement of constant strain rate [8, 11, 58]. Note that, when the strength of the foam is not very low, the profile of incident pulse needs to be modified accordingly to maintain a plateau in reflected pulse [9]. In the SHPB experiment on low-density polymeric foams, dynamic stress equilibrium becomes more critical than constant strain-rate deformation to obtain valid stress-strain data. As mentioned earlier, the foam specimen under non-equilibrated stresses may start to fail from one end (Fig. 3). This phenomenon makes the resultant data unreliable. Therefore, the trapezoidal profile of incident pulse must have a long rise time before the plateau is achieved. The low loading slope allows the specimen to have sufficient time to achieve uniform stress in specimen during early portion of loading. To facilitate such a low-slope trapezoidal incident pulse, both copper tubes and copper disks have been found to effective pulse shapers [8, 9, 11, 58].

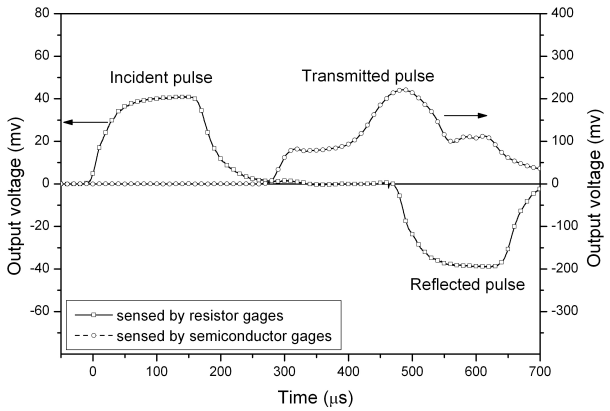

Figure 19: Incident, reflected, and transmitted pulses in a modified SHPB experiment on a polyurethane foam specimen.

Figure 19 shows the typical pulses obtained from a SHPB experiment on a rigid polyurethane foam using a copper tube pulse shaper [58], which displays that a trapezoidal incident pulse with a long rise time was produced. The rise time of the modified incident pulse is approximate 50 μs that is much longer than that ($\sim$10 μs) in a conventional SHPB experiment. The long rise time ensures the early stress equilibrium in such soft materials. It is noted that, due to the severe mechanical impedance mismatch between the foam and the bars material, nearly all the incident

pulse was reflected back as a reflected pulse. The transmitted signal is very weak, although it was sensed by the semiconductor strain gages with a high signal-to-noise ratio. Therefore, the hardening portion behind the stress plateau in the transmitted signal does not significantly affect the design of incident pulse for the purpose of achieving constant strain-rate deformation. The dynamic stress equilibrium process monitored with quartz-crystal force transducers is shown in Fig. 20. An examination of Fig. 20 indicates that, even though the pulse shaper was employed to decrease the incident loading rate, the stress in specimen was not uniform until 50 μs after initial loading, indicating that the initial stress-strain data obtained in the first 50 μs are not reliable. The first 50 μs period covers to approximate 12% strain at this strain rate (4100 s^{-1}), resulting in unreliable elastic and early cell-collapse response for the foam (Fig. 20) [58, 64].

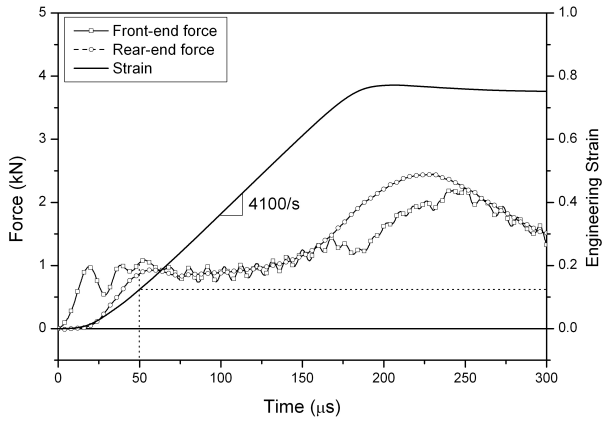

Figure 20: Dynamic stress equilibrium and strain history in the foam specimen.

In order to investigate the initial elastic and early collapse behavior of the material, the initial portion of the incident pulse needs to be precisely controlled [58, 64]. To achieve stress equilibrium earlier in the foam specimen, the loading rate of the incident pulse needs to be lower, which inevitably decreases the strain rate level. When an incident pulse with a lower loading rate, which is shown in Fig. 21, is used, the stress equilibrium is achieved at smaller strains. Figure 22 indicates that the stress equilibrium was achieved at 85 μs after initial loading, which corresponds to only 1.7% strain. In addition, the strain rate had reached to a constant value (450 s^{-1}) when the stress in specimen was in equilibrium. Therefore, the resultant stress-strain curve at the strain rate of 450 s^{-1} shown in Fig. 22 is reliable beyond 1.7% strain. Most of the elastic portion and early collapse portion in the stress-strain curve for the foam material were obtained accurately, although the strain rate was limited in order to achieve valid dynamic testing conditions.

Figure 23 shows the stress-strain curves for the polyurethane foam at various strain rates. As mentioned earlier, the initial elastic and early cell-collapse data are not reliable for the

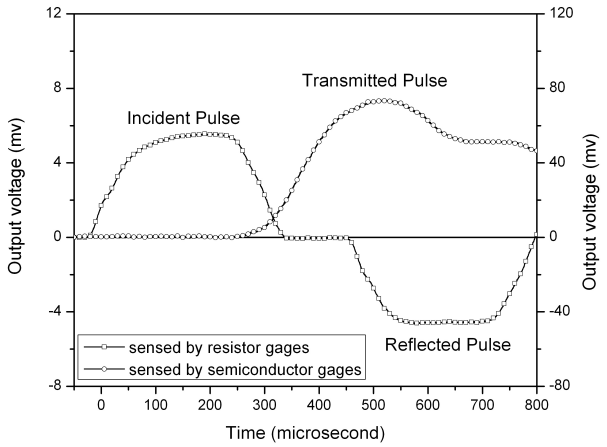

Figure 21: Incident, reflected, and transmitted pulses in a modified SHPB experiment on a polyurethane foam specimen at a lower strain rate.

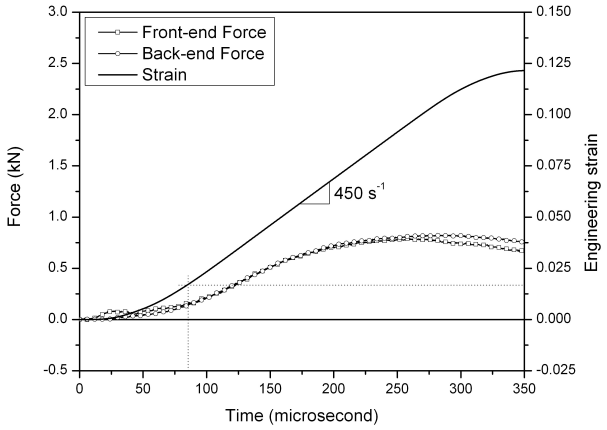

Figure 22: Dynamic stress equilibrium and strain history in the foam specimen at a lower strain rate.

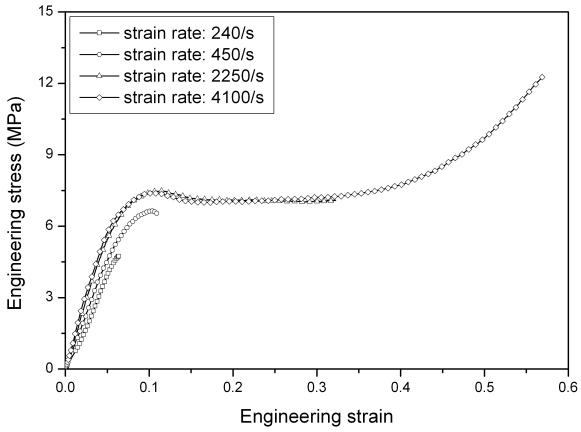

Figure 23: Engineering stress-strain curves of the polyurethane foam at various dynamic strain rates.

experiments at the strain rates of 2250 and 4100 s^{-1}. However, these portions are accurate for the experiments at the strain rates of 240 and 450 s^{-1}. It has been found that there is an upper limit of constant strain rate to obtain reliable stress-strain response for elastic specimens including the elastic-brittle foams as well as the early elastic and cell-collapse response for the regular foam. The estimation of the constant strain-rate limit will be introduced in the following section.

Recently, biological materials such as biological tissues have increasingly investigated. Biological materials, which can be classified as soft materials, may be subjected to impact loading. The high-rate stress-strain response of biological materials is still under investigation. When the SHPB is used to determine stress-strain curves for soft biological materials, the pulse shaping technique is also required to obtain reliable data. The pulse shaping design for testing biological tissues may follow a similar approach as testing soft materials which have similar stress-strain response. For example, bones often exhibit elastic-brittle stress-strain response [44]. Similar to the pulse shaping design for the elastic-brittle foam (epoxy syntactic foam), a nearly linear incident pulse is required to ensure the bone specimen to deform at a nearly constant strain rate under dynamically equilibrated stresses [44]. Skins have been found to exhibit similar stress-strain profiles as rubbers, the pulse shaping design for testing rubbers may be applied to test skins [50]. A porcine skin has been investigated with a pulse-shaped SHPB. The experimental results indicate nonlinear large deformation and rate-sensitive behavior of the porcine skin, which are similar to rubbers [50]. In addition, epoxidized soybean-oil and their nanoclay reinforced composites have been recently experimentally investigated with the pulse-shaping SHPB [59, 60]. Their dynamic compression responses are found to be similar to rubbers too, which exhibit strain-rate-dependent nonlinear large deformations.

In summary, the pulse shaping design is critical to obtain reliable stress-strain data for soft materials deforming at constant strain rates under dynamically equilibrated stresses. The

materials and dimensions of pulse shapers are of many selections as long as the profile of incident pulse is controlled such that a plateau occupies most of the reflected pulse under dynamic stress equilibrium. Varying the material and dimensions of the pulse shaper as well as the striking velocity can produce various amplitudes and profiles of the incident pulses to load the specimen at various constant strain rate levels under dynamically equilibrated stresses.

4 Recent advances in SHPB testing of soft materials

4.1 Upper limit of constant strain rates for testing an elastic specimen with an SHPB

In an experiment, the strain rate in specimen is initially zero and will reach to a constant within a certain amount of time. The strain in specimen is accumulating during this time period. If the failure strain for the specimen is small, the specimen that is loaded at a high strain rate can accumulate significant amount of strain and may fail before the strain rate hikes up to the desired constant level. In this case, the strain rate history in specimen is a ramp profile instead of a plateau, which invalidates the stress-strain data initially targeted to be at a constant strain rate. There exists an upper limit of constant strain rates, beyond which the stress-strain data cannot be obtained at constant strain rates [40].

In their study, Pan et al. [40] used a linear elastic-brittle specimen loaded by a linear ramp incident pulse to estimate the upper limit for constant strain rate. This linear profile of the incident pulse ensures a constant strain rate deformation in the linear elastic specimen. The specimen was assumed to have a certain failure strain independent of strain rate. Based on these assumptions, the upper limit for constant strain rate, $\dot{\varepsilon}_{sc}$, has been obtained and expressed by the following equation

$$\dot{\varepsilon}_{sc} = \frac{2\rho_s A_s C_s^2}{\rho_0 A_0 C_0 L_0} \cdot \frac{1}{\alpha/\eta - 1} \cdot \varepsilon_{sf} \tag{14}$$

where ρ_s, A_s, and C_s are mass density, cross-sectional area, and elastic wave speed in specimen, respectively; ρ_0, A_0, and C_0 are mass density, cross-sectional area, and elastic wave speed in the bars, respectively, as defined previously; L_0 and ε_{sf} are initial length and failure strain of the specimen, respectively. Two constants, α and η, take the following relationship,

$$\eta = 1 - e^{-\alpha} \tag{15}$$

It has been proposed that the strain rate can be considered to be a constant when $\eta = 0.1$, corresponding the value of 2.3 for α. Thus Eq. (14) gives the estimation of upper limit for constant strain rates in an elastic specimen. The upper limits for constant strain-rate estimated by this equation have been verified with experimental results for S-2 glass/SC15 composite and PMMA specimens [40].

It is noted that this upper limit is for the purpose of obtaining constant strain-rate deformation in an elastic specimen. There also exists an upper strain-rate limit for achieving dynamic

stress equilibrium, which was developed by Ravichandran and Subhash [47]. Experimental results indicate that, for the S-2 glass/SC15 composite and PMMA, the upper strain-rate limits to maintain dynamic stress equilibrium are higher than those to maintain constant strain-rate deformation. In this case, the upper limit for constant strain rates becomes more critical. Besides the elastic-brittle materials such as ceramics and composites, the estimation of the upper limit for constant strain rates gives a guideline to design the SHPB experiments on elastic-brittle foams, e.g., epoxy syntactic foam, and regular foams in elastic portions, e.g., polyurethane foam.

4.2 Momentum trapping in SHPB testing for soft materials

To investigate damage evolution in specimen during an SHPB experiment, the specimen needs to be collected for investigation on its microstuctural evolution with tools such as scanning electron microscopy (SEM) or transmission electron microscopy (TEM) examination. In the meantime, the stress/strain history in specimen needs to be accurately understood to develop the relationship between the stress/strain history and damage evolution in specimen. In a conventional SHPB experiment, the specimen may be loaded many times by the pulses reflected back and forth in the incident bar. In this case, the one-to-one correspondence between the microstructural evolution and the loading history in the specimen cannot be established. A single loading on specimen in a SHPB test, which is not automatically produced in a conventional SHPB test, is thus necessary.

A momentum trapping device was originally developed by Nemat-Nasser et al [36, 37] to ensure a single loading in a SHPB experiment. Their design for the dynamic compression test consists of a transfer flange, a tube over the bar, and a reaction mass [36, 37]. The incident tube is placed against the transfer flange at one end and against the reaction mass at the other end. When the striker impacts the transfer flange, it imparts two common compression pulses traveling along the incident tube towards the reaction mass and along the incident bar towards the specimen. The compression pulse in the incident tube is reflected from the reaction mass and travels back to the transfer flange as compression. The compression is reflected from the flange as tension. The tension pulse pulls the incident bar back after first compressive loading on the specimen, avoiding repeated loading on the specimen.

Recently, a simple momentum trapping device was developed [55, 56]. As shown in Fig. 24, this momentum trapping device consists of a flange attached to impact end of incident bar and a rigid mass, through which the incident bar passes, as a momentum trap. A preset gap between the flange and the rigid mass is necessary. This preset gap is precisely controlled such that the gap is just closed when the secondary loading wave reflected from the incident bar arrives. When the gap is closed, the impact of the flange on the rigid mass generates a reverse compressive pulse in the incident bar, which makes the incident bar suddenly stop. When a pulse shaper is placed on the impact end of incident bar, the incident pulse is modified to ensure that the specimen deforms at a nearly constant strain rate under dynamically equilibrated stress. Since the unnecessary momentum is trapped to ensure a single loading on the specimen, the specimen

state under the recorded loading is well defined, which facilitates the possibility to investigate the damage evolution in a specimen, such as a foam specimen.

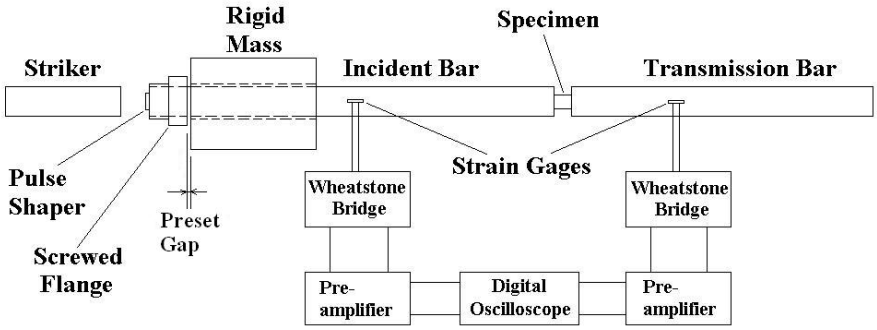

(a)

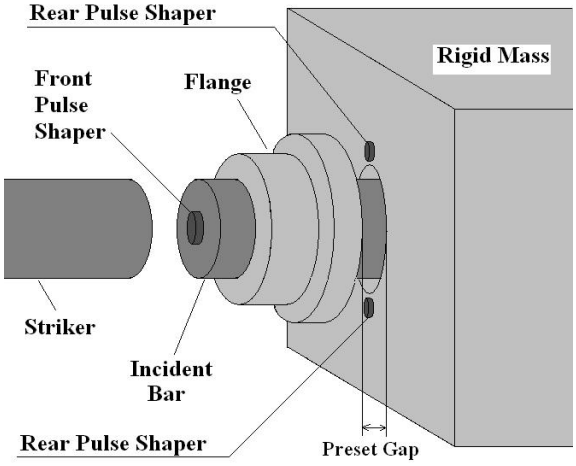

(b)

Figure 24: A schematic of the SHPB with momentum trapping system. a) an overview of the SHPB with the momentum trapping system; b) details of the momentum trapping system.

Figure 25 shows the typical oscilloscope records from the strain gages on incident bar. This figure clearly indicates that the reflected pulse has been reflected back into the incident bar when it traveled to the impact end of incident pulse in a conventional SHPB experiment (Fig. 25). However, this reflected-back pulse was efficiently trapped through the employment of the momentum trapping system as shown in Fig. 25. This momentum trapping system has been used to conduct damage evolutions and compaction wave investigations in foam materials [62,63,65].

It is also noted that, if well-designed pulse shapers (so-called "rear pulse shaper") are placed on the surface of rigid mass, as shown in Fig. 24b, the unloading profile in the incident pulse can also be controlled to ensure that the specimen recovers at the same constant unloading strain

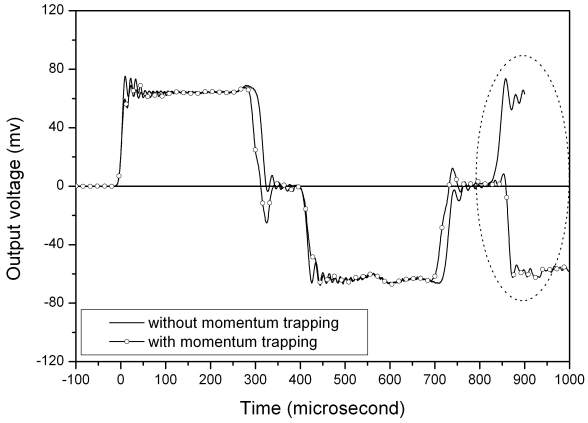

Figure 25: Comparison of pulses obtained from SHPB experiments with and without the momentum trapping system.

rate as the loading strain rate under dynamic stress equilibrium. A dynamic stress-strain loop at the same constant loading and unloading strain rate can thus be obtained [55, 56].

Besides the momentum trapping techniques associated with modifying the incident bar, single loading on the specimen may also be realized by using a shorter and lighter transmission bar or by using strain-limiting collars around the specimen. A shorter transmission bar will leave contact with specimen before arrival of the second loading pulse in the incident bar if the magnitude of the transmitted pulse is reasonably high. A rigid collar around the specimen can stop the incident bar when the specimen is deformed to a desired level and prevent further microstructural changes in the specimen under repeated loading [57].

4.3 Intermediate strain-rate testing of soft materials using SHPB

Soft materials have recently been used in the applications subjected to dynamic loads at not very high rates. For example, strain rates involved in an automotive crash are approximately between 5 and 1000 s^{-1}, and mostly in the lower part below 100 s^{-1} [76,77]. Since a conventional hydraulically-driven materials testing machine is mostly capable of quasi-static experiments at the strain rate up to 10^{-1} s^{-1} whereas an SHPB can load the specimen as low as 10^2 s^{-1}, there exists a strain-rate gap from 10^{-1} to 10^2 s^{-1}, so-called intermediate strain rates, between the quasi-static and Hopkinson bar tests. The needs for accurate stress-strain data at intermediate strain rates have motivated research efforts to develop reliable intermediate strain-rate experimental techniques. The strain rates in drop-weight and Charpy tests may be located in the range of intermediate strain rates. However, these tests cannot provide complete stress-strain curves as a function of strain rate [45, 66], which are necessary for material model development.

Hydraulic testing machines have recently been designed to conduct experiments at interme-

diate strain rates. Due to high actuator speed needed for such experiments, the actuators are typically driven by a larger valve operating at an open-loop mode. However, as discussed earlier, precise control is necessary over the loading history to produce valid data. A better control than an open loop is desired. Attempts have been made to use SHPB to conduct experiments at these strain rates. It is difficult to conduct experiments at intermediate strain rates on soft materials with the SHPB apparatus. One of the challenges is to achieve low striking velocity of the striker bar that is stable and repeatable. Another challenge is that, since soft specimens are capable of very large deformations, the loading duration must be sufficiently long, at intermediate strain rates, to compress the specimens to large strains. At a constant strain rate, the total strain in the specimen is proportional to the pulse duration. To achieve a certain strain level, a longer duration is required at a lower strain rate. The long loading duration inevitably leads to overlapping of the incident and reflected pulses, which are recorded with strain gages on the incident bar, due to limited length of the bars in SHPB experiments.

Zhao and Gary [76,77] utilized periodic round trips of a loading pulse, initially generated by the striker, in the incident bar to load the specimen progressively to large strains. Combining the stress-strain data obtained under each loading provides a full stress-strain curve. They also developed a "slow bar" technique to generate a long loading pulse during one single loading. A device composed of a hydraulic oil jack and a reservoir of compressed air was developed to maintain the pressure to launch the striker. This method theoretically produced a pulse without limitation of duration [76, 77].

Although long incident and transmission bars are desired to record a long loading pulse at relatively low strain rates, it is not realistic to increase the bar length without a limit. The overlapped waves due to insufficient length of bars need to be separated. Methods for wave separation in Hopkinson bar tests have been recently developed [1, 34, 41, 76, 77]. The wave separation in SHPB experiments can be deducted through 2-point strain measurements, where the strain gages are mounted at two different locations on a bar. According to the one-dimensional wave analysis, the overlapped waves can be separated from each other through the measured waves at the two locations.

Once a long loading pulse with desired profile can be is generated, the compression tests on soft materials are feasible for intermediate strain-rate experiments as long as the overlapped waves are separated. Then conventional data reduction is applicable to obtain stress-strain data at intermediate strain rates.

5 Summary

When the Hopkinson bar is used to conduct high-rate experiments on soft materials, the validity of resultant stress-strain data must be carefully examined. Weak transmitted signal, dynamic stress equilibrium, and constant strain-rate deformation are major challenges in obtaining valid stress-strain data for soft materials. The conventional SHPB needs to be properly modified when

it is used for testing soft materials. The modifications to the conventional SHPB are described for soft-material testing in this paper. Besides employing highly sensitive transducers, accurate pulse shaping ensures that the soft specimen deforms at a nearly constant strain rate under dynamically equilibrated stresses. A guideline to pulse shaping design for testing various soft materials with the SHPB is presented. The most recent advances in Hopkinson bar tests of soft materials are also introduced, which include estimation of upper limit in constant strain rate, single-loading techniques, and intermediate strain-rate testing of soft materials.

References

[1] C. Bacon. An experimental method for considering dispersion and attenuation in a viscoelastic hopkinson bar. *Exp. Mech.*, 38:242–249, 1998.

[2] A. M. Bragov and A. K. Lomunov. Methodological aspects of studying dynamic material properties using the kolsky method. *Int. J. Impact Eng.*, 16:321–330, 1995.

[3] D. Casem, T. Weerasooriya, and P. Moy. Inertial effects of quartz force transducers embedded in a split hopkinson pressure bar. *Exp. Mech*, 2005. in press.

[4] D. Casem, T. Weerasooriya, and P. Moy. Acceleration compensation of quartz transducers embedded in a split hopkinson pressure bar. In *Proceedings of the 2003 SEM Annual Conference & Exposition on Experimental and Applied Mechanics*, Charlotte, NC, June 2-4, 2003.

[5] D. T. Casem, W. L. Fourney, and P. Chang. A polymeric split hopkinson pressure bar instrumented with velocity gages. *Exp. Mech.*, 43:420–427, 2003.

[6] W. Chen and F. Lu. A technique for dynamic proportional multiaxial compression on soft materials. *Exp. Mech.*, 40:226–230, 2000.

[7] W. Chen, F. Lu, and M. Cheng. Tension and compression tests of two polymers under quasi-static and dynamic loading. *Polym. Test.*, 21:113–121, 2002.

[8] W. Chen, F. Lu, D. J. Frew, and M. J. Forrestal. Dynamic compression testing of soft materials. asme trans. *J. Appl. Mech.*, 69:214–223, 2002.

[9] W. Chen, F. Lu, and N. Winfree. High-strain-rate compressive behavior of a rigid polyurethane foam with various densities. *Exp. Mech.*, 42:65–73, 2002.

[10] W. Chen, F. Lu, and B. Zhou. A quartz-crystal-embedded split hopkinson pressure bar for soft materials. *Exp. Mech.*, 40:1–6, 2000.

[11] W. Chen and B. Song. Dynamic compression testing on polymeric foams. In *Experiments in Automotive Engineering – Optical Techniques, 2005 SAE World Congress*, Detroit, MI, April 11-14, 2005.

[12] W. Chen, B. Song, D. J. Frew, and M. J. Forrestal. Dynamic small strain measurements of a metal specimen with a split hopkinson pressure bar. *Exp. Mech.*, 43:20–23, 2003.

[13] W. Chen, B. Zhang, and M. J. Forrestal. A split hopkinson bar technique for low-impedance materials. *Exp. Mech.*, 39:81–85, 1999.

[14] W. Chen and B. Zhou. Constitutive behavior of epon 828/t-403 at various strain rates. *Mech. Time-Depend. Mater.*, 2:103–111, 1998.

[15] W. W. Chen, Q. Wu, J. H. Kang, and N. A. Winfree. Compressive superelastic behavior of a niti shape memory alloy at strain rates of 0.001-750 s^{-1}. *Int. J. Solids Struct*, 38:8989–8998, 2001.

[16] R. J. Christensen, S. R. Swanson, and W. S. Brown. Split-hopkinson-bar tests on rocks under confining pressure. *Exp. Mech.*, pages 508–513, November, 1972.

[17] R. Clamroth. Determination of viscoelastic properties by dynamic testing. *Polym. Test.*, 2:263–286, 1981.

[18] N. N. Dioh, P. S. Leevers, and J. G. Williams. Thickness effects in split hopkinson pressure bar tests. *Polymer*, 34:4230–4234, 1993.

[19] J. Duffy, J. D. Campbell, and R. H. Hawley. On the use of a torsional split hopkinson bar to study rate effects in 1100-0 aluminum. *ASME Trans. J. Appl. Mech.*, 37:83–91, 1971.

[20] S. Ellwood, L. J. Griffiths, and D. J. Parry. Materials testing at high constant strain rates. *J. Phys. E: Sci. Instrum.*, 15:280–282, 1982.

[21] C. E. Frantz, P. S. Follansbee, and W. T. Wright. Experimental techniques with the split hopkinson pressure bar. In *Proceedings of the 8^{th} International Conference on High Energy Rate Fabrication*, pages 229–236, Texas, TX, 1984.

[22] D. J. Frew, M. J. Forrestal, and W. Chen. A split hopkinson pressure bar technique to determine compressive stress-strain data for rock materials. *Exp. Mech.*, 41:40–46, 2001.

[23] D. J. Frew, M. J. Forrestal, and W. Chen. Pulse shaping techniques for testing brittle materials with a split hopkinson pressure bar. *Exp. Mech.*, 42:93–106, 2002.

[24] D. J. Frew, M. J. Forrestal, and W. Chen. Pulse shaping techniques for testing elastic-plastic materials with a split hopkinson pressure bar. *Exp. Mech.*, 45:186–195, 2005.

[25] G. T. Gary. Classic split-hopkinson pressure bar testing. mechanical testing and evaluation, metals handbook. *American Society for Metals*, 8:462–476, 2000.

[26] G. T. Gary and W. R. Blumenthal. *Split Hopkinson pressure bar testing of soft materials*, volume 8. American Society for Metals, 2000.

[27] G. T. Gray, W. R. Blumenthal, C. P. Trujillo, and R. W. Carpenter. Influence of temperature and strain rate on the mechanical behavior of adiprene l-100. *J. Phys. IV France Colloque C3 (DYMAT 97)*, 7:523–528, 1997.

[28] J. A. Harris. Dynamic testing under nonsinusoidal conditions and the consequences of nonlinearity for service performance. *Rubber Chem. Technol.*, 60:870–887, 1987.

[29] H. M. Hsiao, I. M. Daniel, and R. D. Cordes. Dynamic compressive behavior of thick composite materials. *Exp. Mech.*, 38:172–180, 1998.

[30] C. H. Karnes and E. A. Ripperger. Strain rate effects in cold worked high-purity aluminum. *J. Mech. Phys. Solids*, 14:75–88, 1966.

[31] H. Kolsky. An investigation of the mechanical properties of materials at very high rates of loading. *Proc. Phys. Soc. London*, B62:676–700, 1949.

[32] W. M. Kriven, B. R. Rosczyk, K. Kremeyer, B. Song, and W. Chen. Transformation toughening of a calcium zirconate matrix by dicalcium silicate under ballistic impact. In W.M. Kriven and H-T Lin, editors, *27th International Cocoa Beach conference on Advanced Ceramics and Composites: A. Ceramic Engineering and Science Proceedings*, volume 24, pages 383–388, 2003.

[33] S. T. Marais, R. B. Tait, T. J. Cloete, and G.N. Nurick. Material testing at high strain rate using the split hopkinson pressure bar. *Latin Amer. J. Solids Struct.*, 1:319–339, 2004.

[34] H. Meng and Q. M. Li. An shpb set-up with reduced time-shift and pressure bar length. *Int. J. Impact Eng.*, 28:677–696, 2003.

[35] M. A. Meyers. *Dynamic Behavior of Materials*. John Wiley & Sons, 1994.

[36] S. Nemat-Nasser. Introduction to high strain rate testing. mechanical testing and evaluation, metals handbook. *American Society for Metals*, 8:427–446, 2000.

[37] S. Nemat-Nasser, J. B. Isaacs, and J. E. Starrett. Hopkinson techniques for dynamic recovery experiments. *Proc. Royal Soc*, 435:371–391, 1991.

[38] L. Ninan, J. Tsai, and C. T. Sun. Use of split hopkinson pressure bar for testing off-axis composites. *Int. J. Impact Eng.*, 25:291–313, 2001.

[39] K. Oguni and G. Ravichandran. Dynamic behavior of fiber reinforced composites under multiaxial compression. In *Thick Composites for Loading Bearing Structures*, pages 87–96. ASME, 1999.

[40] Y. Pan, W. Chen, and B. Song. The upper limit of constant strain rates in a split hopkinson pressure bar experiment with elastic specimens. *Exp. Mech.* accepted.

[41] S. W. Park and M. Zhou. Separation of elastic waves in split hopkinson bars using one-point strain measurements. *Exp. Mech.*, 39:287–294, 1999.

[42] D. J. Parry, P. R. Dixon, S. Hodson, and N. Al-Maliky. Stress equilibrium effects within hopkinson bar experiments. *J. Phys. IV*, C8:107–112, 1994.

[43] P. J. Parry, A. G. Walker, and P. R. Dixon. Hopkinson bar pulse smoothing. *Measurm. Sci. Technol.*, 6:443–446, 1995.

[44] A. Pilcher, X. Wang, G. Niebur, J. Mason, B. Song, M. Cheng, and W. Chen. High strain rate behavior of callellous bone. In *SEM X International Congress and Exposition on Experimental and Applied Mechanics*, Costa Mesa, California, June 7-10, 2004.

[45] R. C. Progelhof. Impact measurement of low-pressure thermoplastic structural foam. In *Proceedings of Instrumented Impact Testing of Plastics and Composite Materials*, pages 105–116, Houston TX, March 11-12, 1986. ASTM.

[46] S. Rao, V. P. W. Shim, and S. E. Quah. Dynamic mechanical properties of polyurethane elastomers using a nonmetallic hopkinson bar. *J. Appl. Polym. Sci.*, 66:619–631, 1997.

[47] G. Ravichandran and G. Subhash. Critical appraisal of limiting strain rates for compression resting of ceramics in a split hopkinson pressure bar. *J. Am. Ceram. Soc.*, 77:263–267, 1994.

[48] S. Sarva and S. Nemat-Nasser. Dynamic compressive strength of silicon carbide under uniaxial compression. *Mater. Sci. Eng.*, A317:140–144, 2001.

[49] O. Sawas, N. S. Brar, and R. A. Brockman. Dynamic characterization of compliant materials using an all-polymeric split hopkinson bar. *Exp. Mech.*, 38:204–210, 1998.

[50] O. A. Shergold, N. A. Fleck, and D. Radford. The uniaxial stress versus strain response of pig skin and silicone rubber at low and high strain rates. *Int. J. Impact Eng.*, 2005. in press.

[51] B. Song and W. Chen. One-dimensional dynamic compressive behavior of epdm rubber. *AME Trans. J. Eng. Mater. Technol.*, 125:294–301, 2003.

[52] B. Song and W. Chen. Dynamic compressive behavior of epdm rubber under nearly uniaxial strain conditions. *ASME Trans. J. Eng. Mater. Technol.*, 126:213–217, 2004.

[53] B. Song and W. Chen. Dynamic compressive behavior of epdm rubber under nearly uniaxial strain conditions. *ASME Trans. J. Eng. Mater. Technol.*, 126:213–217, 2004.

[54] B. Song and W. Chen. Dynamic stress equilibration in split hopkinson pressure bar tests on soft materials. *Exp. Mech.*, 44:300–312, 2004.

[55] B. Song and W. Chen. Loading and unloading shpb pulse shaping techniques for dynamic hysteretic loops. *Exp. Mech.*, 44:622–627, 2004.

[56] B. Song and W. Chen. A shpb pulse shaping technique for dynamic stress-strain loops. In *Proceedings of the 2004 SEM X International Congress & Exposition on Experimental and Applied Mechanics*, Costa Mesa, California, USA, June 7-10, 2004.

[57] B. Song, W. Chen, and D. J. Frew. Quasi-static and dynamic compressive and failure behaviors of an epoxy syntactic foam. *J. Compos. Mater.*, 38:915–936, 2004.

[58] B. Song, W. Chen, and X. Jiang. Split hopkinson pressure bar experiments on polymeric foams. *Int. J. Vehicle Des.*, 37:185–198, 2005.

[59] B. Song, W. Chen, Z. Liu, and S. Z. Erhan. Compressive properties of epoxidized soybean-oil/clay nanocomposites. *Int. J. Plasticity.* submitted.

[60] B. Song, W. Chen, Z. Liu, and S. Z. Erhan. Compressive properties of soybean-oil based polymers at quasi-static and dynamic strain rates. *J. Appl. Polym. Sci.*, 2005. in press.

[61] B. Song, W. Chen, and T. Weerasooriya. Quasi-static and dynamic compressive behaviors of a s-2 glass/sc15 composite. *J. Compos. Mater.*, 37:1723–1743, 2003.

[62] B. Song, W. Chen, T. Yanagita, and D. J. Frew. Confinement effects on dynamic compressive properties of an epoxy syntactic foam. *Compos. Struct.*, 67:279–287, 2005.

[63] B. Song, W. Chen, T. Yanagita, and D. J. Frew. Temperature effects on dynamic compressive behavior of an epoxy syntactic foam. *Compos. Struct.*, 67:289–298, 2005.

[64] B. Song, W. W. Chen, S. Dou, N. A. Winfree, and J. H. Kang. Strain-rate effects on elastic and early cell-collapse responses of a polystyrene foam. *Int. J. Impact Eng.*, 31:509–521, 2005.

[65] B. Song, M. J. Forrestal, and W. Chen. Dynamic and quasi-static propagation of compaction waves in a low density epoxy foam. *Exp. Mech.* accepted.

[66] D. F. Sounik, P. Gansen, J. L. Clemons, and J. W. Liddle. Head-impact testing of polyurethane energy-absorbing (ea) foams. *SAE Trans. J. Mater. & Manu.*, 106:211–220, 1997.

[67] G. Subhash, R. J. Dowding, and L. J. Kecskes. Characterization of uniaxial compressive response of bulk amorphous zr-ti-cu-ni-be alloy. *Mater. Sci. Eng.*, A334:33–40, 2002.

[68] G. Subhash and G. Ravichandran. *Split-Hopkinson pressure bar testing of ceramics. Mechanical Testing and Evaluation, Metals Handbook*, volume 8. American Society for Metals, 2000.

[69] T. C. Togami, W. E. Baker, and M. J. Forrestal. A split hopkinson pressure bar technique to evaluate the performance of accelerometers. *ASME Trans. J. Appl. Mech.*, 63:353–356, 1996.

[70] L. Wang, K. Labibes, Z. Azari, and G. Pluvinage. Generalization of split hopkinson bar technique to use viscoelastic bars. *Int. J. Impact Eng.*, 15:669–686, 1994.

[71] R. J. Wasley, K. G. Hoge, and J. C. Cast. Combined strain gauge-quartz crystal instrumented hopkinson split bar. *Rev. Sci. Instrum.*, 40:889–894, 1969.

[72] R. G. Whirley and J. O. Hallquist. *DYNA3D: A nonlinear, explict, three-dimensional finite element code for solid and structural mechanics – user manual. UCRL-MA-107254.* Lawrence Livermore National Laboratory, Livermore, California, 1991.

[73] X. J. Wu and D. A. Gorham. Stress equilibrium in the split hopkinson pressure bar test. *J. Phys. IV France*, C3:91–96, 1997.

[74] U. Zencker and R. Clos. Limiting conditions for compression testing of flat specimens in the split hopkinson pressure bar. *Exp. Mech.*, 39:343–348, 1998.

[75] H. Zhao and G. Gary. A three dimensional analytical solution of the longitudinal wave propagation in an infinite linear viscoelastic cylindrical bar: application to experimental techniques. *J. Mech. Phys. Solids*, 43:1335–1348, 1995.

[76] H. Zhao and G. Gary. A new method for separation of waves. application to the shpb technique for an unlimited measuring duration. *J. Mech. Phys. Solids*, 45:1185–1202, 1997.

[77] H. Zhao and G. Gary. Behaviour characterization of polymeric foams over a large range of strain rates. *Int. J. Vehicle Des.*, 30:135–145, 2002.

[78] H. Zhao, G. Gary, and J. R. Klepaczko. On the use of a viscoelastic split hopkinson pressure bar. *Int. J. Impact Eng.*, 19:319–330, 1997.

[79] J. A. Zukas, T. Nicholas, H. F. Swift, L. B. Greszczuk, and D. R. Curran. *Impact Dynamics.* Krieger Publishing Company, 1992.